

000 001 002 003 004 005 OFMU: OPTIMIZATION-DRIVEN FRAMEWORK FOR 006 MACHINE UNLEARNING 007 008 009

010 **Anonymous authors**
011 Paper under double-blind review
012
013
014
015
016
017
018
019
020
021
022
023
024
025
026
027
028
029
030

031 ABSTRACT 032

033 Large language models deployed in sensitive applications increasingly require the
034 ability to *unlearn* specific knowledge, such as user requests, copyrighted materials,
035 or outdated information, without retraining from scratch to ensure regulatory
036 compliance, user privacy, and safety. This task, known as machine unlearning,
037 aims to remove the influence of targeted data (*forgetting*) while maintaining per-
038 formance on the remaining data (*retention*). A common approach is to formulate
039 this as a multi-objective problem and reduce it to a single-objective prob-
040 lem via scalarization, where forgetting and retention losses are combined using
041 a weighted sum. However, this often results in unstable training dynamics and
042 degraded model utility due to conflicting gradient directions. To address these
043 challenges, we propose **OFMU**, a penalty-based bi-level optimization framework
044 that explicitly prioritizes forgetting while preserving retention through a hier-
045 archical structure. Our method enforces forgetting via an inner maximization step
046 that incorporates a similarity-aware penalty to decorrelate the gradients of the for-
047 get and retention objectives, and restores utility through an outer minimization
048 step. To ensure scalability, we develop a two-loop algorithm with provable conver-
049 gence guarantees under both convex and non-convex regimes. We further provide
050 a rigorous theoretical analysis of convergence rates and show that our approach
051 achieves better trade-offs between forgetting efficacy and model utility compared
052 to prior methods. Extensive experiments across vision and language benchmarks
053 demonstrate that OFMU consistently outperforms existing unlearning methods in
054 both forgetting efficacy and retained utility.

055 1 INTRODUCTION 056

057 Large language models (LLMs) have become foundational to applications ranging from search en-
058 gines and coding assistants to healthcare, education, and scientific discovery. Their remarkable
059 performance arises from training on massive and diverse corpora, which inevitably contain sensi-
060 tive, copyrighted, or harmful information. This raises serious concerns about privacy, regulatory
061 compliance, safety, and ethics. In particular, regulations such as the General Data Protection Regu-
062 lation (GDPR) (European Union, 2016; California Legislative Counsel, 2018; Office of the Privacy
063 Commissioner of Canada, 2018) grant individuals the “right to be forgotten” (Dang, 2021) requiring
064 deployed models to eliminate the influence of specific data upon request. Beyond regulatory man-
065 dates, unlearning is also necessary to prevent models from generating toxic content, leaking private
066 information, or providing instructions for misuse (Huang et al., 2022; Carlini et al., 2023; Staab
067 et al., 2024). These considerations have led to growing interest in *machine unlearning*, the ability to
068 selectively erase the impact of particular data from a trained model while maintaining its utility.

069 **Limitations of Existing Approaches.** Existing unlearning methods for LLMs can be broadly cat-
070 egorized into three families (see Appendix 7.6 for a broader discussion): input-based, data-based,
071 and model-based approaches. Input-based methods modify the prompts or instructions given to the
072 model so that it refuses to generate content related to the forget set (Pawelczyk et al., 2023; Liu
073 et al., 2024b). These methods are lightweight but typically brittle, as adversarial prompts can of-
074 ten bypass the refusal policy. Data-based methods fine-tune the model on curated examples that
075 encourage desirable outputs when queried with forget-related prompts (Choi et al., 2024). While
076 effective in narrow settings, such methods risk semantic distortion, require careful construction of
077 auxiliary data, and may not generalize beyond specific domains. Model-based approaches directly

alter model parameters through techniques such as fine-tuning, gradient ascent, or projection (Bu et al., 2024; Fan et al., 2024; 2025; Dong et al., 2024; Zhang et al., 2024b). These approaches are generally more effective at suppressing unwanted knowledge, but they introduce a deeper optimization challenge: balancing the trade-off between forgetting the targeted information and preserving utility on the retain set.

Most model-based methods formulate this balance as a scalarized optimization problem, where the forget loss and retain loss are combined with fixed weights into a single objective. This design leads to several shortcomings. First, static weighting fails to reflect the dynamic nature of unlearning: early optimization steps should prioritize forgetting, while later updates should shift emphasis toward restoring utility. However, fixed weights cannot adapt accordingly. Second, scalarization is inherently unstable. When the forget objective dominates, the model can collapse, leading to severe performance degradation on the retain set. When the retain objective dominates, forgetting remains incomplete and sensitive data can persist. Third, most existing algorithms perform poorly on *hard-to-unlearn samples* (see Appendix 7.5.6), where forget and retain gradients are strongly entangled. In such cases, aggressive updates on the forget set cause disproportionate collateral damage to the retain set, as evidenced by the strong coupling between sample difficulty and utility loss. Figure 1 further shows that while many methods perform adequately on *easy-to-unlearn* samples, their performance drops sharply as difficulty increases. This trend underscores their inability to maintain stable performance under challenging conditions, ultimately failing to meet the true objective of unlearning. Finally, existing approaches largely lack principled theoretical grounding, instead relying on heuristic weighting schemes that scale poorly in the high-dimensional, non-convex optimization landscapes of modern LLMs.

These challenges call for a more principled and structured approach to optimization-based unlearning, one that recognizes the asymmetric priorities of forgetting and retention. Crucially, *forgetting must take precedence*. If a model fails to unlearn harmful content, its retained capabilities are irrelevant from a safety or compliance perspective. In contrast, once forgetting is successful, utility can be gradually restored as long as the erased information does not re-emerge. This observation motivates a hierarchical optimization view, where forgetting is posed as a primary inner objective, and retention is addressed as a secondary outer goal.

Our Approach: OFMU. We introduce **OFMU** (Optimization-Driven Framework for Machine Unlearning), a penalty-based bi-level optimization framework that formalizes this hierarchy. OFMU addresses the shortcomings of existing methods through three key innovations: (i) a principled penalty-based reformulation that enforces stationarity of the inner forgetting objective, enabling efficient two-loop optimization without requiring full convergence of the inner problem; (ii) a similarity-aware penalty that explicitly decorrelates gradients between forget and retain objectives, mitigating destructive interference during updates; and (iii) a rigorous convergence analysis of penalty-based unlearning under both convex and non-convex regimes.

Contributions. Our main contributions are summarized as follows:

- We propose OFMU, a novel optimization-driven bi-level framework that explicitly prioritizes forgetting over utility preservation, capturing the conceptual hierarchy inherent in unlearning.
- We develop a scalable two-loop algorithm with provable convergence guarantees, avoiding the computational bottlenecks of traditional bi-level optimization methods.
- We design a similarity-aware penalty that dynamically decorrelates forget and retain gradients, ensuring that forgetting does not inadvertently degrade retained knowledge.

- 108 • We provide a comprehensive theoretical analysis of convergence rates for penalty-based unlearning
109 in both convex and non-convex settings.
- 110 • We empirically validate OFMU across benchmark unlearning tasks in language and vision models,
111 establishing a new state-of-the-art in the forgetting-utility trade-off.

113 2 BI-LEVEL OPTIMIZATION IN MACHINE LEARNING

115 Bi-level optimization has emerged as a powerful paradigm for problems where two interdependent
116 objectives must be optimized in a hierarchical manner. Formally, it consists of an *outer* optimization
117 task whose feasible solutions are implicitly constrained by the optimal solutions of an *inner* optimi-
118 zation problem (Colson et al., 2007; Dempe & Zemkoho, 2020). This nested structure provides
119 a natural way to capture tasks where one objective has strict priority over another, such as hyperpa-
120 rameter tuning (Franceschi et al., 2018), meta-learning (Finn et al., 2017; Nichol et al., 2018), and
121 adversarial robustness (Madry et al., 2018).

122 Recent advances have demonstrated the utility of bi-level optimization in large-scale machine learn-
123 ing, particularly in domains where competing goals must be balanced without collapsing into triv-
124 ial solutions. For instance, in meta-learning, the inner problem adapts to specific tasks, while the
125 outer problem promotes generalization across tasks (Hospedales et al., 2021). Similarly, in adver-
126 sarial training, the inner maximization crafts adversarial perturbations, and the outer minimization
127 strengthens the model against them (Zhang et al., 2019). These successes highlight the versatil-
128 ity of the framework in structuring inherently asymmetric objectives and avoid trivial or unstable
129 solutions.

130 We adopt this perspective for machine unlearning. In this setting, forgetting must be enforced as
131 a non-negotiable objective, ensuring that the influence of target data is fully removed, while utility
132 preservation is treated as a secondary goal to be optimized conditionally. This stands in contrast to
133 scalarized approaches that conflate the two objectives via fixed weights, often leading to brittle trade-
134 offs. Bi-level optimization, by explicitly separating the two, allows us to respect the asymmetry of
135 their importance and design algorithms that reflect this priority structure. This foundational insight
136 motivates our proposed framework, OFMU, which we formally present in Section 3.

137 3 METHODOLOGY

138 We now present the OFMU framework, a penalty-based bi-level optimization method that explicitly
139 separates the forgetting and utility preservation objectives. We begin by introducing notation and
140 formalizing the problem, then describe the bi-level formulation, its penalty-based reformulation, and
141 our scalable two-loop algorithm.

143 3.1 PRELIMINARIES AND NOTATION

144 We consider a supervised learning setup with a dataset $\mathcal{D} = \mathcal{D}_r \cup \mathcal{D}_f$, where \mathcal{D}_r is the *retain*
145 set (examples to be preserved) and \mathcal{D}_f is the *forget* set (examples to be unlearned). The model is
146 denoted by f_θ , parameterized by $\theta \in \mathbb{R}^d$.

147 **Empirical Losses.** We define the empirical losses over each subset as:

$$149 \mathcal{L}_r(\theta) = \frac{1}{|\mathcal{D}_r|} \sum_{(x,y) \in \mathcal{D}_r} \ell(f_\theta(x), y), \quad \mathcal{L}_f(\theta) = \frac{1}{|\mathcal{D}_f|} \sum_{(x,y) \in \mathcal{D}_f} \ell(f_\theta(x), y), \quad (1)$$

153 where $\ell(\cdot, \cdot)$ is a standard loss function (e.g., cross-entropy).

154 **Gradients and Similarity.** We denote the gradients of the retain and forget losses as $\nabla_\theta \mathcal{L}_r(\theta)$ and
155 $\nabla_\theta \mathcal{L}_f(\theta)$, respectively. To quantify their alignment, we use cosine similarity:

$$157 \text{Sim}(\nabla_\theta \mathcal{L}_f, \nabla_\theta \mathcal{L}_r) = \frac{\langle \nabla_\theta \mathcal{L}_f, \nabla_\theta \mathcal{L}_r \rangle}{\|\nabla_\theta \mathcal{L}_f\| \|\nabla_\theta \mathcal{L}_r\|}, \quad (2)$$

160 which captures directional alignment, abstracting away differences in magnitude. In the context of
161 unlearning, this is crucial: if $\nabla_\theta \mathcal{L}_r(\theta)$ and $\nabla_\theta \mathcal{L}_f(\theta)$ are highly aligned, forgetting updates may
162 interfere with retention, motivating decorrelation.

162 **Penalty Parameter.** To ensure tractability, we will use a penalty parameter $\rho > 0$, which enforces
 163 the stationarity condition of the inner maximization through a soft constraints. This allows us to
 164 avoid solving the inner problem to completion while still preserving its structure.

165 A full notation summary is provided in Appendix 7.1 which will be used throughout the paper.

167 3.2 PROBLEM SETUP

168 The goal of machine unlearning is to remove the influence of the forget set \mathcal{D}_f from a trained model,
 169 while preserving performance on the retain set \mathcal{D}_r . Formally, we seek model parameters θ such that
 170 the model’s predictions are independent of \mathcal{D}_f , yet its performance on \mathcal{D}_r remains optimal.

171 However, these objectives are often in conflict: naively increasing the loss on \mathcal{D}_f can significantly
 172 degrade utility on \mathcal{D}_r . To address this, we introduce a bi-level optimization framework that explicitly
 173 separates the forgetting and utility objectives. The inner problem seeks to maximize forgetting and
 174 decorrelate the influence of \mathcal{D}_f and \mathcal{D}_r via a similarity penalty, while the outer problem restores
 175 utility on \mathcal{D}_r . The resulting bi-level optimization problem is:

$$176 \min_{\theta \in \mathbb{R}^d} \mathcal{L}_r(\theta) \quad \text{subject to} \quad \theta \in \arg \max_{\theta' \in \mathbb{R}^d} [\mathcal{L}_f(\theta') - \beta \cdot \text{Sim}(\nabla_{\theta} \mathcal{L}_f(\theta'), \nabla_{\theta} \mathcal{L}_r(\theta'))], \quad (3)$$

178 where $\beta > 0$ controls the strength of the gradient decorrelation penalty. For ease of presentation,
 179 we define

$$180 \Phi(\theta) := \mathcal{L}_f(\theta) - \beta \cdot \text{Sim}(\nabla_{\theta} \mathcal{L}_f(\theta), \nabla_{\theta} \mathcal{L}_r(\theta)). \quad (4)$$

182 The formulation in equation 3 ensures that:

- 183 • The inner maximization emphasizes forgetting on \mathcal{D}_f while decorrelating from \mathcal{D}_r .
- 184 • The outer minimization restores utility on \mathcal{D}_r , subject to the constraint that forgetting has already
 185 been enforced.

186 3.3 BI-LEVEL FORMULATION

188 We now explicitly separate the two objectives via bi-level optimization.

189 **Inner Maximization (Forgetting and Decorrelation).** The inner problem seeks parameters that
 190 maximize the loss on the forget set while minimizing the similarity between the gradients of the
 191 forget and retain losses. This is achieved by solving:

$$193 \theta_{\text{in}}^* = \arg \max_{\theta'} [\Phi(\theta')]. \quad (5)$$

195 **Outer Minimization (Utility Restoration).** Given the solution θ_{in}^* from the inner problem, the
 196 outer problem seeks to minimize the loss on the retain set:

$$197 \theta^* = \arg \min_{\theta \leftarrow \theta_{\text{in}}^*} \mathcal{L}_r(\theta). \quad (6)$$

200 **Stationarity Constraint.** The bi-level structure enforces that the final model parameters θ^* are
 201 stationary points of the inner maximization objective, i.e., $\nabla_{\theta} \Phi(\theta^*) = 0$.

202 3.4 PENALTY-BASED SINGLE-LEVEL REFORMULATION

204 Directly solving the bi-level optimization problem is computationally challenging, especially for
 205 large-scale models, due to repeated inner maximization and higher-order derivatives computation.
 206 To address this, we adopt a penalty-based single-level reformulation that transforms the bi-level
 207 problem into a tractable unconstrained optimization.

208 **Penalty Reformulation.** We introduce a penalty term that enforces the stationarity condition of
 209 the inner maximization as a soft constraint. The resulting objective is:

$$210 F(\theta) = \mathcal{L}_r(\theta) + \rho \|\nabla_{\theta} \Phi(\theta)\|^2, \quad (7)$$

212 where $\Phi(\theta) = \mathcal{L}_f(\theta) - \beta \cdot \text{Sim}(\nabla_{\theta} \mathcal{L}_f(\theta), \nabla_{\theta} \mathcal{L}_r(\theta))$ and $\rho > 0$ penalizes deviation from stationarity.
 213 As ρ increases, the penalty term forces θ to approach the stationary point of the inner objective $\Phi(\theta)$.
 214 In the limit as $\rho \rightarrow \infty$, any minimizer of $F(\theta)$ satisfies the original bi-level constraint $\nabla_{\theta} \Phi(\theta) = 0$.
 215 This formulation transforms a nested optimization into a tractable single-level objective while
 preserving the hierarchical structure.

216

3.5 PRACTICAL ALGORITHM AND IMPLEMENTATION

217

218 The penalty-based OFMU algorithm is designed for scalability and efficiency in large-scale deep
 219 learning settings. Although the penalty reformulation converts the original bi-level problem into a
 220 single-level objective, directly optimizing the full loss landscape can be unstable and computationally
 221 inefficient. To address this, we adopt a two-loop optimization scheme that alternates between
 222 maximizing forgetting and minimizing penalized retain loss. Here, we describe the motivation for
 223 this design, its computational advantages, and the implementation details.

224

225 **Motivation for Two-Loop Optimization.** While the penalty-based reformulation enables direct
 226 optimization of a single objective, the landscape of $F(\theta) = \mathcal{L}_r(\theta) + \rho \|\nabla_\theta \Phi(\theta)\|^2$ can be highly non-
 227 convex, especially for deep models. A naive approach may struggle to find good stationary points,
 228 especially in the presence of conflicting gradient signals from forgetting and retention. The two-
 229 loop scheme mitigates this issue by explicitly maximizing the inner objective $\Phi(\theta)$, which captures
 230 both the forget loss and the gradient decorrelation penalty, before each outer update. This design
 231 has two key benefits: (i) it encourages the model to traverse regions of the parameter space that are
 232 explicitly optimized for forgetting. (ii) it improves stability and convergence by warm-starting each
 233 outer iteration from a locally optimized initialization.

234

235 Importantly, in the non-convex setting typical of deep learning, the theoretical guarantee is conver-
 236 gence to a stationary point of the penalty objective $F(\theta)$. This point corresponds to a local minimum,
 237 maximum, or saddle point. However, because the inner objective $\Phi(\theta)$ is maximized using gradient
 238 ascent, the algorithm is biased toward stationary points that are local maxima of the inner objective,
 239 which aligns with the unlearning goal. This type of guarantee is the strongest possible in general
 240 non-convex optimization and is standard in the literature for deep learning and LLMs.

241

242 In contrast, the original bi-level formulation requires fully solving the inner maximization to conver-
 243 gence at each outer iteration, which is computationally prohibitive for large models. Our proposed
 244 approach avoids this bottleneck while still enforcing the desired stationarity constraint. For example,
 245 in LLMs, a full bi-level update may require thousands of inner steps or even retraining, whereas our
 246 approach typically uses a small, fixed T (e.g., $T = 5$ or 10), dramatically reducing compute cost.

247

248 **Two-Loop Optimization Scheme.** At each outer iteration k , the algorithm alternates between:

249

250 **1. Inner Loop (Forgetting Maximization):** Starting from the current parameters $\theta^{(k)}$, run T steps
 251 of gradient ascent on the inner objective $\Phi(\theta)$ to increase the forget loss while decorrelating it
 252 from retain gradients:

253

$$\theta'^{(t+1)} = \theta'^{(t)} + \eta_{\text{in}} \nabla_\theta \Phi(\theta'^{(t)}), \quad t = 0, \dots, T-1, \quad (8)$$

254

255 where η_{in} is the inner learning rate and $\theta'^{(0)} = \theta^{(k)}$. The final inner iterate $\theta_{\text{in}}^{(k)} = \theta'^{(T)}$ serves as
 256 the initialization for the outer loop.

257

258 **2. Outer Loop (Utility Preservation with Penalty):** The outer step minimizes the retain loss $\mathcal{L}_r(\theta)$
 259 while enforcing the stationarity condition of the inner objective $\Phi(\theta)$. Formally, the update is
 260 given by

261

$$\theta^{(k+1)} = \theta_{\text{in}}^{(k)} - \eta_{\text{out}} \nabla_\theta F(\theta_{\text{in}}^{(k)}), \quad (9)$$

262

263 where η_{out} is the outer learning rate, and $\nabla_\theta F(\theta_{\text{in}}^{(k)}) = \nabla_\theta \mathcal{L}_r(\theta_{\text{in}}^{(k)}) + 2\rho_k \nabla_\theta^2 \Phi(\theta_{\text{in}}^{(k)}) \nabla_\theta \Phi(\theta_{\text{in}}^{(k)})$.

264

265 Here, ρ_k is the penalty parameter at iteration k , $\nabla_\theta \Phi$ is the gradient of the inner objective, and $\nabla_\theta^2 \Phi$
 266 is its Hessian. The second term, $2\rho_k \nabla_\theta^2 \Phi \nabla_\theta \Phi$, results from differentiating the term $\rho_k \|\nabla_\theta \Phi(\theta)\|^2$
 267 with respect to θ , which requires computing a Hessian-vector product (see Appendix 7.7 for details
 268 on its efficient computation via automatic differentiation).

269

270 **Penalty Schedule and Practical Considerations.** A growing penalty parameter gradually
 271 strengthens the enforcement of the inner stationarity condition $\nabla_\theta \Phi(\theta) = 0$. In practice, we adopt
 272 an increasing schedule $\rho_{k+1} > \rho_k$: smaller values stabilize the early iterations, while larger values
 273 amplify the term $\rho_k \|\nabla_\theta \Phi(\theta)\|^2$, ensuring that violations of stationarity become progressively more
 274 costly. A formal justification of this property is provided later in Lemma 1.

275

276 **Mini-Batch Stochastic Gradients.** To ensure scalability, all gradients are approximated using
 277 mini-batches sampled independently from \mathcal{D}_f and \mathcal{D}_r denoted as \mathcal{B}_f and \mathcal{B}_r , each of size B . The
 278 stochastic gradient estimations $\nabla_\theta \mathcal{L}_f(\theta; \mathcal{B}_f)$ and $\nabla_\theta \mathcal{L}_r(\theta; \mathcal{B}_r)$ reduce the per-iteration computa-
 279 tional cost from $O(|\mathcal{D}|)$ to $O(B)$, thereby enabling training on large-scale datasets. While stochastic-
 280 ity introduces variance into the gradient estimates, our two-loop formulation remains robust due

270 **Algorithm 1** Penalty-Based OFMU Bi-Level Unlearning

271 **Require:** Initial parameters $\theta^{(0)}$, penalty schedule $\{\rho_k\}_{k=0}^K$, regularization $\beta > 0$, learning rates
 $\eta_{\text{in}}, \eta_{\text{out}}$, number of outer iterations K , number of inner steps T , batch size B

272 **Require:** Datasets: \mathcal{D}_f (forget set), \mathcal{D}_r (retain set)

273 1: **for** $k = 0, 1, \dots, K - 1$ **do**

274 2: **(Inner maximization: Forgetting)**

275 3: Initialize $\theta'^{(0)} \leftarrow \theta^{(k)}$

276 4: **for** $t = 0, 1, \dots, T - 1$ **do**

277 5: Sample mini-batch $\mathcal{B}_f \subset \mathcal{D}_f$, $\mathcal{B}_r \subset \mathcal{D}_r$ of size B

278 6: Compute $\nabla_{\theta'} \mathcal{L}_f(\theta'^{(t)}; \mathcal{B}_f)$ and $\nabla_{\theta'} \mathcal{L}_r(\theta'^{(t)}; \mathcal{B}_r)$

279 7: Compute $\text{Sim}(\nabla_{\theta} \mathcal{L}_f, \nabla_{\theta} \mathcal{L}_r)$

280 8: $\Phi(\theta'^{(t)}) \leftarrow \mathcal{L}_f(\theta'^{(t)}; \mathcal{B}_f) - \beta \cdot \text{Sim}(\nabla_{\theta} \mathcal{L}_f, \nabla_{\theta} \mathcal{L}_r)$

281 9: $\theta'^{(t+1)} \leftarrow \theta'^{(t)} + \eta_{\text{in}} \nabla_{\theta'} \Phi(\theta'^{(t)})$ ▷ Gradient ascent

282 10: **end for**

283 11: **(Outer minimization: Utility preservation with penalty)**

284 12: Set $\theta_{\text{in}}^{(k)} \leftarrow \theta'^{(T)}$

285 13: Sample mini-batch $\mathcal{B}'_r \subset \mathcal{D}_r$ of size B

286 14: Compute $\nabla_{\theta} \mathcal{L}_r(\theta_{\text{in}}^{(k)}; \mathcal{B}'_r)$

287 15: Compute $\nabla_{\theta} \Phi(\theta_{\text{in}}^{(k)})$ and $\nabla_{\theta}^2 \Phi(\theta_{\text{in}}^{(k)}) \nabla_{\theta} \Phi(\theta_{\text{in}}^{(k)})$

288 16: $\theta^{(k+1)} \leftarrow \theta_{\text{in}}^{(k)} - \eta_{\text{out}} \left(\nabla_{\theta} \mathcal{L}_r(\theta_{\text{in}}^{(k)}; \mathcal{B}'_r) + 2\rho_k \nabla_{\theta}^2 \Phi(\theta_{\text{in}}^{(k)}) \nabla_{\theta} \Phi(\theta_{\text{in}}^{(k)}) \right)$ ▷ Gradient descent

289 17: Update penalty: $\rho_{k+1} \leftarrow \text{Increase}(\rho_k)$

290 18: **end for**

291 19: **Output:** Final parameters $\theta^{(K)}$

295 to the penalty term $\|\nabla_{\theta} \Phi(\theta)\|^2$, which regularizes the updates and stabilizes convergence. Algorithm 1 formally presents the complete OFMU process, which terminates after a fixed number of
296 outer iterations or once the stationarity criterion is reached.

4 THEORETICAL ANALYSIS

301 We now provide theoretical analysis for the penalty-based bi-level formulation introduced in Section 3. Our analysis establishes theoretical guarantees for the OFMU algorithm, showing that: (i)
302 the penalty reformulation enforces the stationarity condition on the forgetting objective, (ii) the inner
303 maximization step converges under standard assumptions, and (iii) the full two-loop algorithm
304 converges in both convex and non-convex settings. **We further provide a separate analysis of the**
305 **computational complexity of OFMU in Appendix 7.4.** These results provide the theoretical foundation
306 for OFMU and validate its design choices.

308 **Penalty Reformulation Enforces Stationarity.** We first show that the penalty-based single-level
309 reformulation of the bi-level unlearning problem enforces stationarity of the inner objective, i.e.,
310 $\nabla_{\theta} \Phi(\theta) = 0$, as the penalty parameter ρ increases. This result, presented in following lemma with
311 the proof in Appendix 7.2.1 motivates the use of the penalty method in OFMU.

312 **Lemma 1** (Stationarity via Penalty Reformulation). *Let \mathcal{L}_r and Φ be continuously differentiable
313 and bounded below. For any sequence $\{\theta_{\rho}^*\}$ of minimizers of $F(\theta) = \mathcal{L}_r(\theta) + \rho \|\nabla_{\theta} \Phi(\theta)\|^2$ with
314 $\rho \rightarrow \infty$, every accumulation point θ^* satisfies $\nabla_{\theta} \Phi(\theta^*) = 0$.*

315 **Convergence of the Inner Maximization Step.** Next lemma, with the proof provided in Ap-
316 pendix 7.2.2 analyzes the convergence of the inner maximization loop, showing that gradient ascent,
317 which is used to maximize $\Phi(\theta)$ achieves sublinear convergence in the convex setting.

318 **Lemma 2** (Convergence Inner Maximization). *Let $\Phi(\theta)$ be convex and differentiable with L -
319 Lipschitz continuous gradient. Then, applying T steps of gradient ascent: $\theta'^{(t+1)} = \theta'^{(t)} +$
320 $\eta_{\text{in}} \nabla \Phi(\theta'^{(t)})$ with step size $0 < \eta_{\text{in}} \leq 1/L$ yields the bound:*

$$\Phi(\theta_{\text{in}}^*) - \Phi(\theta'^{(T)}) \leq \frac{\|\theta_{\text{in}}^* - \theta'^{(0)}\|^2}{2T\eta_{\text{in}}},$$

321 where $\theta_{\text{in}}^* = \arg \max_{\theta} \Phi(\theta)$.

324 **Convergence of the Full Two-Loop Algorithm.** Finally, we establish convergence guarantees for
 325 the penalty-based OFMU algorithm in both convex and non-convex regimes in the following lemma
 326 with the proof provided in Appendix 7.3.

327 **Lemma 3** (Convergence of Penalty-Based OFMU). *Under Assumptions 7.3, the penalty-based
 328 OFMU algorithm converges in both convex and non-convex settings:*

329 • **Convex case:** If $\mathcal{L}_r(\theta)$ and $\Phi(\theta)$ are convex and L -smooth, then after K outer iterations with T
 330 inner steps per iteration, the suboptimality satisfies

$$332 \quad F(\theta^{(K)}) - F^* \leq \mathcal{O}\left(\frac{1}{K}\right) + \mathcal{O}\left(\frac{K}{T^2}\right).$$

334 Setting $K, T = \mathcal{O}(1/\epsilon)$ ensures ϵ -optimality of the penalty objective.

335 • **Non-convex case:** If either $\mathcal{L}_r(\theta)$ or $\Phi(\theta)$ is non-convex but L -smooth, then OFMU converges to
 336 an ϵ -stationary point of $F(\theta)$, with the expected squared gradient norm bounded by

$$337 \quad \min_{k=0, \dots, K-1} \mathbb{E}\|\nabla F(\theta^{(k)})\|^2 \leq \mathcal{O}\left(\frac{1}{K}\right) + \mathcal{O}\left(\frac{1}{T}\right) + \mathcal{O}(\sigma^2),$$

339 where σ^2 captures the variance of stochastic gradients.

341 5 EXPERIMENTS

343 In this section, we describe the experimental setup and evaluate our proposed method, **OFMU**,
 344 on both language and vision tasks to assess its effectiveness and generality. Our experiments are
 345 designed to examine three key aspects: (i) whether OFMU achieves strong unlearning efficacy while
 346 preserving model utility in LLMs; (ii) how OFMU compares against state-of-the-art unlearning
 347 baselines across different benchmarks; and (iii) whether OFMU extends effectively to non-language
 348 tasks such as vision-based classification.

349 5.1 EXPERIMENTAL SETUP

351 We conduct all experiments on two NVIDIA H100 80GB GPUs and two NVIDIA H100 NVL 96GB
 352 GPUs. For LLMs, we consider two widely used benchmarks: (i) **TOFU** (Maini et al., 2024b), a
 353 synthetic QA dataset on fictitious authors designed to test entity-level unlearning; (ii) **WMDP** (Li
 354 et al., 2024), which evaluates unlearning in high-stakes domains such as biosecurity, cybersecurity,
 355 and chemical safety. For vision tasks, we use **CIFAR-10** and **CIFAR-100** (Krizhevsky & Hinton,
 356 2009) and evaluate OFMU under two settings: (i) class-wise forgetting, where all examples from
 357 one or more classes are removed and (ii) random forgetting, where a randomly selected subset
 358 spanning all classes is removed. Sections 5.2 and 5.3 present results on the **TOFU** and **CIFAR-10**
 359 benchmarks respectively, while results for **WMDP** and **CIFAR-100**, together with complete details
 360 of the experimental setup, evaluation metrics, baselines, and models, are deferred to Appendix 7.5.

361 5.2 TOFU RESULTS

362 For TOFU benchmark, we evaluate OFMU across three forgetting scenarios: `forget01`,
 363 `forget05`, and `forget10`, which correspond to removing 1%, 5%, and 10% of
 364 the dataset, respectively, using two model architectures: `LLaMA-2-7B-hf-chat`¹ and
 365 `LLaMA-3.2-1B-Instruct`². We report performance using three key metrics: forget quality
 366 (FQ), model utility (MU), and forget truth ratio (FTR), where higher values indicate more effective
 367 forgetting, better utility retention, and stronger reliability of unlearned outputs, respectively.

368 **Forgetting Quality.** On both architectures, OFMU achieves strong FQ, comparable to or exceeding
 369 preference-based methods such as NPO (Bourtoule et al., 2021). In `forget01`, OFMU achieves
 370 slightly lower FQ than NPO on LLaMA-2 but matches or surpasses it on LLaMA-3.2, while main-
 371 taining stronger MU and FTR. This highlights that our framework prioritizes balance rather than
 372 over-optimizing a single metric. Unlike Gradient Ascent (GA) (Thudi et al., 2022) and Gradient
 373 Difference (GD) (Maini et al., 2024a), which aggressively maximize the forget loss but collapse to
 374 near-zero utility, OFMU enforces forgetting without destabilizing updates.

375 **Utility Preservation.** MU is where many baselines diverge. Methods like RMU (Li et al., 2024) pre-
 376 serve utility well but at the cost of incomplete forgetting, while GA achieves near-perfect forgetting

377 ¹<https://huggingface.co/meta-llama/Llama-2-7b-chat-hf>

²https://huggingface.co/open-unlearning/tofu_Llama-3.2-1B-Instruct_full

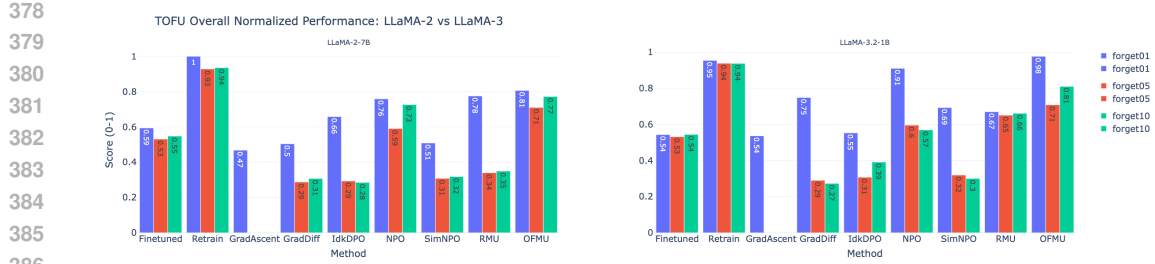


Figure 2: Overall normalized performance of unlearning methods on LLaMA-2 and LLaMA-3 under different forget scenarios (1%, 5%, 10%). The overall score is computed by normalizing FQ, MU, and FTR and then averaging them. Higher scores indicate better balance between forgetting efficacy and utility preservation. Detail about calculation is provided in Appendix 7.5.3

but eliminates MU entirely. In `forget05`, although GA attains higher raw FQ, its utility completely collapses ($MU = 0.00$), whereas OFMU sustains competitive FQ with substantially higher MU (0.65 on LLaMA-2). Similarly, in `forget10`, OFMU preserves robustness across all metrics, while GA and GD sacrifice utility entirely, and NPO degrades sharply. Overall, OFMU maintains MU close to the Retain baseline while still enforcing strong forgetting.

Truth Ratio. FTR further confirms OFMU’s balanced behavior. Whereas GA and GD degrade truthfulness due to unstable optimization, and NPO variants sometimes inflate FTR by overfitting to retain data. OFMU consistently maintains high FTR across all scenarios. This indicates that unlearned models continue to provide reliable responses, rather than memorized or distorted ones.

Table 1: Performance of unlearning methods on TOFU using LLaMA-2-7B-hf-chat and LLaMA-3.2-1B-Instruct under different forget scenarios.

Method	LLaMA-2-7B-hf-chat						LLaMA-3.2-1B-Instruct								
	forget01			forget05			forget10			forget01			forget05		
	FQ↑	MU↑	FTR↑	FQ↑	MU↑	FTR↑	FQ↑	MU↑	FTR↑	FQ↑	MU↑	FTR↑	FQ↑	MU↑	FTR↑
Finetuned	1.27e-03	0.63	0.53	5.87e-14	0.63	0.51	4.35e-25	0.63	0.52	0.01	0.60	0.47	1.33e-13	0.60	0.47
Retrain	1.00	0.63	0.68	1.00	0.63	0.67	1.00	0.61	0.68	1.00	0.60	0.65	1.00	0.64	1.00
GradAscent	1.88e-04	0.55	0.36	1.94e-119	0.00	8.82e-96	1.06e-239	0.00	2.21e-32	0.27	0.33	0.59	1.94e-119	0.00	2.52e-23
GradDiff	3.02e-03	0.57	0.41	1.94e-119	0.56	4.14e-95	1.80e-229	0.58	1.46e-07	0.77	0.43	0.57	1.94e-119	0.53	3.87e-34
IdkDPO	0.10	0.56	0.67	4.02e-06	0.04	0.67	5.42e-13	0.04	0.64	0.01	0.51	0.60	1.12e-05	0.07	0.62
NPO	0.40	0.58	0.65	0.09	0.53	0.71	0.42	0.54	0.73	0.92	0.56	0.66	0.14	0.45	0.70
SimNPO	1.27e-03	0.58	0.41	1.06e-106	0.60	3.94e-05	1.47e-198	0.60	3.17e-04	0.58	0.46	0.55	5.01e-100	0.58	4.19e-03
RMU	0.40	0.62	0.64	9.59e-10	0.02	0.81	6.92e-21	0.03	0.81	0.16	0.55	0.70	4.87e-10	0.58	0.77
OFMU (ours)	0.42	0.63	0.68	0.13	0.65	0.82	0.41	0.61	0.76	0.93	0.61	0.74	0.15	0.61	0.75

To capture a holistic view of unlearning efficacy, we aggregate the three core metrics — FQ, MU, FTR into a single normalized score (Figure 2). This unified view highlights the balance between forgetting and retention across different forget scenarios and shows how OFMU strikes the balance to achieve overall better results in unlearning.

5.3 CIFAR-10 RESULTS

For CIFAR-10, we evaluate OFMU under two settings: *class-wise forgetting*, where an entire class is removed, and *random forgetting*, where 10% of the training data is randomly selected as the forget set. The results are summarized in Table 2. We report Unlearning Accuracy (UA), Retain Accuracy (RA), Total Accuracy (TA), and Membership Inference Attack efficacy (MIA-Efficacy), where higher values indicate better unlearning performance and robustness.

Class-wise Forgetting. Retraining from scratch achieves perfect unlearning (100% UA) and strong overall utility (94.80% RA, 91.82% TA), but is com-

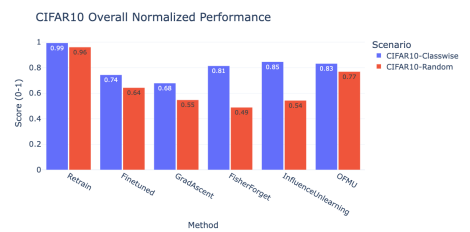


Figure 3: Overall normalized performance of unlearning methods on CIFAR-10. The score is obtained by normalizing four key metrics—UA, RA, TA, and MIA Efficacy—within each scenario and averaging them into a unified value. Details of the calculation are given in Appendix 7.5.3.

putationally infeasible. Among approximate methods, Fisher Forget (FF) (Golatkar et al., 2021) and Influence Unlearning (IU) (Mehta et al., 2022) preserve utility reasonably well, with IU in particular showing the highest UA (89.31%). However, IU is computationally expensive, requiring repeated influence function estimations and parameter adjustments, which makes it impractical for LLMs with billions of parameters. In contrast, OFMU achieves a balanced trade-off: 81.51% UA, 93.51% RA, and 86.88% TA. While its UA is slightly lower than IU, OFMU generalizes more effectively, as shown by its higher MIA-Efficacy (59.76). This indicates that OFMU not only forgets the targeted class but also improves robustness against membership inference attacks, a critical security measure. Unlike IU, OFMU scales naturally to deep non-convex settings without prohibitive computational cost, making it more suitable for practical deployment in LLMs.

Random Forgetting. The random forgetting task is more challenging, since the forget set is dispersed rather than concentrated. Retraining achieves the highest UA (6.79%), while most approximate methods collapse, with UA close to zero (e.g., GA: 0.78%, FF: 0.51%). These methods struggle to generalize forgetting uniformly across the randomly distributed forget samples, highlighting their sensitivity to the structure of the forget set. OFMU achieves 7.71% UA, slightly outperforming retraining. While its RA (92.25%) and TA (88.61%) are marginally lower than retrain or fine-tuning, OFMU maintains a better balance by reducing susceptibility to membership inference (MIA-Efficacy: 3.36 versus 1.21 and 1.87 for FF and GA, respectively). This shows that OFMU enforces forgetting more uniformly, even in the scattered random setting, without collapsing utility.

Table 2: **Performance of unlearning methods on CIFAR-10 under class-wise and random forgetting.**
Values show mean \pm standard deviation over 5 runs.

Method	Class-wise Forgetting			MIA \uparrow	Random Forgetting (10% forget set)			
	UA \uparrow	RA \uparrow	TA \uparrow		UA \uparrow	RA \uparrow	TA \uparrow	MIA \uparrow
Retrain	100.00 \pm 0.0	94.80 \pm 0.2	91.82 \pm 0.3	100.00 \pm 0.0	6.79 \pm 0.3	100.00 \pm 0.0	92.04 \pm 0.1	16.08 \pm 0.5
Finetuned (FT)	42.43 \pm 2.1	94.19 \pm 0.5	94.61 \pm 0.6	56.51 \pm 2.8	1.82 \pm 0.2	99.54 \pm 0.2	92.84 \pm 0.4	5.66 \pm 0.4
GradAscent (GA)	37.11 \pm 2.2	86.52 \pm 1.7	82.41 \pm 2.0	55.03 \pm 2.7	0.78 \pm 0.3	99.38 \pm 0.3	92.10 \pm 0.7	1.87 \pm 0.4
Fisher Forget (FF)	79.71 \pm 1.4	94.12 \pm 0.4	93.96 \pm 0.6	46.38 \pm 2.4	0.51 \pm 0.2	88.03 \pm 1.8	87.70 \pm 1.9	1.21 \pm 0.4
Influence Unlearning (IU)	89.31 \pm 1.1	92.19 \pm 0.7	90.63 \pm 1.0	55.22 \pm 2.5	0.62 \pm 0.3	99.39 \pm 0.3	94.43 \pm 0.6	1.51 \pm 0.3
OFMU (ours)	81.51 \pm 1.3	93.51 \pm 0.6	86.88 \pm 1.2	59.76 \pm 2.4	7.71 \pm 0.4	92.25 \pm 0.9	88.61 \pm 1.1	3.36 \pm 0.6

The CIFAR-10 results further underscore the robustness of OFMU. Whereas existing baselines overemphasize either unlearning or retention, OFMU achieves stable performance across both scenarios, validating the advantages of its hierarchical optimization design. As shown in Figure 3, we also report the overall normalized score for CIFAR-10, analogous to the TOFU benchmark. In the class-wise setting, Influence Unlearning (IU) attains higher unlearning accuracy, but its heavy computational cost limits practicality. In the more challenging random forgetting scenario, where most baselines collapse, OFMU achieves the best overall performance. These results confirm that OFMU maintains a consistent balance across metrics, achieving effective and robust unlearning without sacrificing generalization, unlike methods that over-optimize for a single objective.

6 CONCLUSION AND FUTURE WORK

In this work, we introduced **OFMU**, a penalty-based bi-level framework for machine unlearning that explicitly prioritizes forgetting before utility preservation. By combining a scalable two-loop algorithm with a similarity-aware penalty, OFMU achieves state-of-the-art trade-offs across language and vision benchmarks. Our theoretical analysis provides convergence guarantees in convex and non-convex regimes, and empirical results consistently demonstrate improved stability, robustness to hard-to-forget samples, and stronger resilience against membership inference attacks compared to existing approaches.

Although OFMU makes significant progress, several directions remain open. First, extending OFMU to continual unlearning scenarios, where multiple requests arrive sequentially, would enhance its applicability. Second, investigating adaptive penalty schedules and alternative gradient similarity measures could further improve robustness. Finally, applying OFMU to even larger foundation models and diverse modalities such as speech and multimodal learning presents a promising avenue for future research.

REFERENCES

Ludovic Bourtoule, Varun Chandrasekaran, Christopher A. Choquette-Choo, Haoran Jia, Adam Travers, Bita Zhang, David Lie, and Nicolas Papernot. Machine unlearning. In *2021 IEEE Sympo-*

486 *sium on Security and Privacy (SP)*, pp. 141–159. IEEE, 2021. doi: 10.1109/SP40001.2021.00030.
 487

488 Zhiqi Bu, Xiaomeng Jin, Bhanukiran Vinzamuri, Anil Ramakrishna, Kai-Wei Chang, Volkan
 489 Cevher, and Mingyi Hong. Unlearning as multi-task optimization: A normalized gradient dif-
 490 ference approach with an adaptive learning rate. *arXiv preprint arXiv:2410.22086*, 2024.

491 California Legislative Counsel. Bill text, california consumer privacy act (ab-375).
 492 [https://leginfo.legislature.ca.gov/faces/billTextClient.xhtml?
 493 bill_id=201720180AB375](https://leginfo.legislature.ca.gov/faces/billTextClient.xhtml?bill_id=201720180AB375), 2018. Accessed: 2025-09-16.

494 Yinzhi Cao and Junfeng Yang. Towards making systems forget with machine unlearning. In *2015*
 495 *IEEE Symposium on Security and Privacy*, pp. 463–480. IEEE, 2015. doi: 10.1109/SP.2015.35.
 496

497 Nicholas Carlini, Daphne Ippolito, Matthew Jagielski, Katherine Lee, Florian Tramèr, and Chiyuan
 498 Zhang. Quantifying memorization across neural language models. In *The Eleventh International*
 499 *Conference on Learning Representations (ICLR)*, Kigali, Rwanda, May 2023. OpenReview.net.

500 Jiaao Chen and Diyi Yang. Unlearn what you want to forget: Efficient unlearning for llms. *arXiv*
 501 *preprint arXiv:2310.20150*, 2023.
 502

503 Minseok Choi, Daniel Rim, Dohyun Lee, and Jaegul Choo. Snap: Unlearning selective knowledge
 504 in large language models with negative instructions. *arXiv preprint arXiv:2406.12329*, 2024.

505 Benoît Colson, Patrice Marcotte, and Gilles Savard. An overview of bilevel optimization. *Annals of*
 506 *Operations Research*, 153(1):235–256, 2007. doi: 10.1007/s10479-007-0176-2.
 507

508 Quang-Vinh Dang. Right to be forgotten in the age of machine learning. In *Advances in Digital*
 509 *Science: ICADS 2021*, pp. 403–411. Springer, 2021.

510 Stephan Dempe and Alain B. Zemkoho. *Bilevel Optimization: Advances and Next Challenges*.
 511 Springer, 2020. doi: 10.1007/978-3-030-52119-6.
 512

513 Yijiang River Dong, Hongzhou Lin, Mikhail Belkin, Ramon Huerta, and Ivan Vulic. Undial: Self-
 514 distillation with adjusted logits for robust unlearning in large language models. *arXiv preprint*
 515 *arXiv:2402.10052*, 2024.

516 Ronen Eldan and Mark Russinovich. Who's harry potter? approximate unlearning in llms. *arXiv*
 517 *preprint arXiv:2310.02238*, 2023.
 518

519 European Union. General data protection regulation (gdpr), 2016. URL <https://eur-lex.europa.eu/eli/reg/2016/679/oj>. Regulation (EU) 2016/679.
 520

521 Chongyu Fan, Jiancheng Liu, Licong Lin, Jinghan Jia, Ruiqi Zhang, Song Mei, and Sijia Liu. Sim-
 522 plicity prevails: Rethinking negative preference optimization for llm unlearning. *arXiv preprint*
 523 *arXiv:2410.07163*, 2024.

524 Chongyu Fan, Jiancheng Liu, Licong Lin, Jinghan Jia, Ruiqi Zhang, Song Mei, and Sijia Liu. Sim-
 525 plicity prevails: Rethinking negative preference optimization for llm unlearning. 2025.
 526

527 Chelsea Finn, Pieter Abbeel, and Sergey Levine. Model-agnostic meta-learning for fast adaptation
 528 of deep networks. In *Proceedings of the 34th International Conference on Machine Learning (ICML)*, 2017. URL <http://proceedings.mlr.press/v70/finn17a.html>.
 529

530 Luca Franceschi, Michele Donini, Paolo Frasconi, and Massimiliano Pontil. Bilevel programming
 531 for hyperparameter optimization and meta-learning. In *Proceedings of the 35th International Con-
 532 ference on Machine Learning (ICML)*, 2018. URL <http://proceedings.mlr.press/v80/franceschi18a.html>.
 533

534 Aditya Golatkar, Alessandro Achille, Avinash Ravichandran, Marco Polito, and Stefano Soatto.
 535 Mixed-privacy forgetting in deep networks. In *Proceedings of the IEEE/CVF Conference on*
 536 *Computer Vision and Pattern Recognition (CVPR)*, pp. 792–801, 2021.
 537

538 Timothy M. Hospedales, Antreas Antoniou, Paul Micaelli, and Amos J. Storkey. Meta-learning in
 539 neural networks: A survey. *IEEE Transactions on Pattern Analysis and Machine Intelligence*, 44
 (9):5149–5179, 2021. doi: 10.1109/TPAMI.2021.3079209.

540 James Y. Huang, Wenxuan Zhou, Fei Wang, Fred Morstatter, Sheng Zhang, Hoifung Poon, and
 541 Muhao Chen. Offset unlearning for large language models. *Transactions on Machine Learning*
 542 *Research*, May 2025.

543

544 Jie Huang, Hanyin Shao, and Kevin Chen-Chuan Chang. Are large pre-trained language models
 545 leaking your personal information? In *Findings of the Association for Computational Linguistics: EMNLP 2022*, pp. 2038–2047, Abu Dhabi, United Arab Emirates, December 2022. Association for Computational Linguistics.

546

547 Jinghan Jia, Jiancheng Liu, Parikshit Ram, Yuguang Yao, Gaowen Liu, Yang Liu, Pranay Sharma,
 548 and Sijia Liu. Model sparsity can simplify machine unlearning. In *Advances in Neural Information Processing Systems (NeurIPS)*, 2023. URL <https://doi.org/10.48550/arXiv.2304.04934>. Spotlight.

549

550

551

552 Anastasia Koloskova, Youssef Allouah, Animesh Jha, Rachid Guerraoui, and Sanmi Koyejo. Certified
 553 unlearning for neural networks. In *Proceedings of the 42nd International Conference on Machine Learning*, volume 267 of *Proceedings of Machine Learning Research*, Vancouver, Canada, 2025. PMLR.

554

555

556 Alex Krizhevsky and Geoffrey Hinton. Learning multiple layers of features from tiny images. Technical report, University of Toronto, 2009. Technical Report.

557

558

559 Nathaniel Li, Alexander Pan, Anjali Gopal, Summer Yue, Daniel Berrios, Alice Gatti, Justin D. Li,
 560 Ann-Kathrin Dombrowski, Shashwat Goel, Long Phan, Gabriel Mukobi, Nathan Helm-Burger,
 561 Rassim Lababidi, Lennart Justen, Andrew B. Liu, Michael Chen, Isabelle Barrass, Oliver Zhang,
 562 Xiaoyuan Zhu, Rishabh Tamirisa, Bhrugu Bharathi, Adam Khoja, Zhenqi Zhao, Ariel Herbert-Voss,
 563 Cort B. Breuer, Samuel Marks, Oam Patel, Andy Zou, Mantas Mazeika, Zifan Wang,
 564 Palash Oswal, Weiran Lin, Adam A. Hunt, Justin Tienken-Harder, Kevin Y. Shih, Kemper Talley,
 565 John Guan, Russell Kaplan, Ian Steneker, David Campbell, Brad Jokubaitis, Alex Levinson, Jean
 566 Wang, William Qian, Kallol Krishna Karmakar, Steven Basart, Stephen Fitz, Mindy Levine, Pon-
 567 nurangam Kumaraguru, Uday Tupakula, Vijay Varadharajan, Ruoyu Wang, Yan Shoshtaishvili,
 568 Jimmy Ba, Kevin M. Esvelt, Alexander Wang, and Dan Hendrycks. The wmdp benchmark: Mea-
 569 suring and reducing malicious use with unlearning. *arXiv preprint arXiv:2403.03218*, 2024.

570

571 Chris Yuhao Liu, Yaxuan Wang, Jeffrey Flanigan, and Yang Liu. Large language model unlearning
 572 via embedding-corrupted prompts. *arXiv preprint arXiv:2406.07933*, 2024a.

573

574 Chris Yuhao Liu, Yaxuan Wang, Jeffrey Flanigan, and Yang Liu. Large language model unlearning
 575 via embedding-corrupted prompts. *arXiv preprint arXiv:2406.07933*, 2024b.

576

577 Aleksander Madry, Aleksandar Makelov, Ludwig Schmidt, Dimitris Tsipras, and Adrian Vladu.
 578 Towards deep learning models resistant to adversarial attacks. In *International Conference on Learning Representations (ICLR)*, 2018. URL <https://openreview.net/forum?id=rJzIBfZAb>.

579

580 Pratyush Maini, Zhili Feng, Avi Schwarzschild, Zachary C Lipton, and J Zico Kolter. Tofu: A task
 581 of fictitious unlearning for llms. *arXiv preprint arXiv:2401.06121*, 2024a.

582

583 Pratyush Maini, Zhili Feng, Avi Schwarzschild, Zachary C. Lipton, and J. Zico Kolter. Tofu: A
 584 task of fictitious unlearning for llms. In *International Conference on Learning Representations (ICLR)*, 2024b.

585

586 Ronak Mehta, Siddharth Pal, Vivek Singh, and S. N. Ravi. Deep unlearning via randomized condi-
 587 tionally independent hessians. In *Proceedings of the IEEE/CVF Conference on Computer Vision and Pattern Recognition (CVPR)*, pp. 10412–10421, 2022.

588

589 Anmol Mekala, Vineeth Dorna, Shreya Dubey, Abhishek Lalwani, David Koleczek, Mukund
 590 Rungta, Sadid Hasan, and Elita Lobo. Alternate preference optimization for unlearning factual
 591 knowledge in large language models. *arXiv preprint arXiv:2409.13474*, 2024.

592

593 Yizhong Meng, Mengzhou Xia, and Danqi Chen. Simpo: Simple preference optimization with a
 594 reference-free reward. In *Advances in Neural Information Processing Systems (NeurIPS)*, volume 37, pp. 124198–124235, 2024.

594 Andrei Muresanu, Anvith Thudi, Michael R Zhang, and Nicolas Papernot. Unlearnable algorithms
 595 for in-context learning. *arXiv preprint arXiv:2402.00751*, 2024.

596

597 Alex Nichol, Joshua Achiam, and John Schulman. Reptile: A scalable meta-learning algorithm.
 598 <https://arxiv.org/abs/1803.02999>, 2018. arXiv:1803.02999.

599

600 Office of the Privacy Commissioner of Canada. Announcement: Privacy commissioner seeks federal
 601 court determination on key issue for canadians' online reputation. https://www.priv.gc.ca/en/opc-news/news-and-announcements/2018/an_181010/, Oct 2018. Ac-
 602 cessed: 2025-09-16.

603

604 Martin Pawelczyk, Seth Neel, and Himabindu Lakkaraju. In-context unlearning: Language models
 605 as few shot unlearners. *arXiv preprint arXiv:2310.07579*, 2023.

606

607 Barak A. Pearlmutter. Fast exact multiplication by the hessian. In *Neural Computation*, volume 6,
 608 pp. 147–160. MIT Press, 1994.

609

610 Robin Staab, Mark Vero, Mislav Balunovic, and Martin T. Vechev. Beyond memorization: Violating
 611 privacy via inference with large language models. In *The Twelfth International Conference on
 Learning Representations (ICLR)*, Vienna, Austria, May 2024. OpenReview.net.

612

613 Anvith Thudi, Gabriel Deza, Varun Chandrasekaran, and Nicolas Papernot. Unrolling sgd: Un-
 614 derstanding factors influencing machine unlearning. In *2022 IEEE 7th European Symposium on
 Security and Privacy (EuroS&P)*, pp. 303–319. IEEE, 2022.

615

616 Yuanshun Yao, Xiaojun Xu, and Yang Liu. Large language model unlearning. *arXiv preprint
 arXiv:2310.10683*, 2023.

617

618 Binchi Zhang, Yushun Dong, Tianhao Wang, and Jundong Li. Towards certified unlearning for
 619 deep neural networks. In *Proceedings of the 41st International Conference on Machine Learning
 (ICML)*, volume 235 of *Proceedings of Machine Learning Research*, Vienna, Austria, 2024a.
 620 PMLR.

621

622 Chenlong Zhang, Zhuoran Jin, Hongbang Yuan, Jiaheng Wei, Tong Zhou, Kang Liu, Jun Zhao,
 623 and Yubo Chen. Rule: Reinforcement unlearning achieves forget-retain pareto optimality. *arXiv
 preprint arXiv:2506.07171*, 2025. Accepted at NeurIPS 2025.

624

625 Hongyang Zhang, Yaodong Yu, Jiantao Jiao, Eric P. Xing, Laurent El Ghaoui, and Michael I. Jordan.
 626 Theoretically principled trade-off between robustness and accuracy. In *Proceedings of the 36th
 International Conference on Machine Learning (ICML)*, 2019. URL <http://proceedings.mlr.press/v97/zhang19p.html>.

627

628 R. Zhang, L. Lin, Y. Bai, and S. Mei. Negative preference optimization: From catastrophic collapse
 629 to effective unlearning. In *Conference on Learning on Large Language Models (COLM)*, 2024b.

630

631 Jakub Łucki, Boyi Wei, Yangsibo Huang, Peter Henderson, Florian Tramèr, and Javier Rando. An
 632 adversarial perspective on machine unlearning for ai safety. *arXiv preprint arXiv:2409.18025*,
 633 2024.

634

635

636

637 **7 APPENDIX**

638

639 **7.1 NOTATION SUMMARY**

640

- $\theta \in \mathbb{R}^d$: model parameters.
- $\mathcal{D} = \mathcal{D}_r \cup \mathcal{D}_f$: full dataset.
- \mathcal{D}_r : retain set (data to preserve).
- \mathcal{D}_f : forget set (data to unlearn).
- $\ell(\cdot, \cdot)$: base loss function (e.g., cross-entropy).
- $\mathcal{L}_r(\theta)$: empirical loss on the retain set.
- $\mathcal{L}_f(\theta)$: empirical loss on the forget set.
- $\Phi(\theta) = \mathcal{L}_f(\theta) - \beta \cdot \text{Sim}(g_f, g_r)$: inner maximization objective.

- $F(\theta) = \mathcal{L}_r(\theta) + \rho \|\nabla_\theta \Phi(\theta)\|^2$: penalty-based reformulated objective.
- $\nabla_\theta \mathcal{L}_r(\theta)$: gradient of the retain loss.
- $\nabla_\theta \mathcal{L}_f(\theta)$: gradient of the forget loss.
- $\text{Sim}(\nabla_\theta \mathcal{L}_f(\theta), \nabla_\theta \mathcal{L}_r(\theta))$: cosine similarity between $\nabla_\theta \mathcal{L}_f(\theta)$ and $\nabla_\theta \mathcal{L}_r(\theta)$.
- $\nabla_\theta^2 \Phi(\theta)$: Hessian of the inner objective.
- Hv : Hessian–vector product (Pearlmutter trick).
- $\beta > 0$: regularization parameter for similarity-aware decorrelation.
- $\rho > 0$: penalty parameter enforcing stationarity.
- η_{in} : learning rate for the inner loop.
- η_{out} : learning rate for the outer loop.
- T : number of inner loop steps per outer iteration.
- K : number of outer iterations.
- B : mini-batch size.
- $\theta_{\text{in}}^{(k)}$: parameters after inner loop at iteration k .
- $\theta^{(k)}$: parameters after outer loop at iteration k .
- FQ: Forget Quality (lower residual accuracy on forget set).
- MU: Model Utility (performance on retain set).
- FTR: Forget Truth Ratio (faithfulness of unlearning).
- UA: Unlearning Accuracy (CIFAR evaluation).
- RA: Retain Accuracy.
- TA: Total Accuracy.
- MIA-Efficacy: Membership Inference Attack efficacy.
- UDI(x): Unlearning Difficulty Index for sample x .
- $\|\nabla_\theta \mathcal{L}_{\text{forget}}(x)\|_2$: gradient norm of forget loss on x .
- $\Delta\ell(x)$: loss margin to the target threshold (used in UDI).
- $\tau(\cdot, \cdot)$: Spearman correlation coefficient.

7.2 LEMMA PROOFS

7.2.1 PROOF OF LEMMA 1

Proof. Let θ_ρ^* be a minimizer of $F(\theta) = \mathcal{L}_r(\theta) + \rho \|\nabla_\theta \Phi(\theta)\|^2$ for a given $\rho > 0$. Assume \mathcal{L}_r and Φ are continuously differentiable and bounded below.

Suppose, for contradiction, that there exists an accumulation point θ^* of the sequence $\{\theta_\rho^*\}$ as $\rho \rightarrow \infty$ such that $\nabla_\theta \Phi(\theta^*) \neq 0$. Then, for sufficiently large ρ , the penalty term $\rho \|\nabla_\theta \Phi(\theta_\rho^*)\|^2$ would dominate $F(\theta_\rho^*)$, causing it to diverge to infinity, which contradicts the assumption that $F(\theta_\rho^*)$ is minimized and bounded below.

Therefore, it must be that $\nabla_\theta \Phi(\theta^*) = 0$ for any accumulation point θ^* of the minimizers as $\rho \rightarrow \infty$. \square

7.2.2 PROOF OF LEMMA 2

Proof. Let $d^{(t)} := \theta_{\text{in}}^* - \theta'^{(t)}$. By convexity of Φ , for any θ and θ^* ,

$$\Phi(\theta^*) \leq \Phi(\theta) + \langle \nabla \Phi(\theta), \theta^* - \theta \rangle, \quad (10)$$

so

$$\Phi(\theta_{\text{in}}^*) - \Phi(\theta'^{(t)}) \leq \langle \nabla \Phi(\theta'^{(t)}), d^{(t)} \rangle. \quad (11)$$

The update rule gives:

$$d^{(t+1)} = d^{(t)} - \eta_{\text{in}} \nabla \Phi(\theta'^{(t)}), \quad (12)$$

so

$$\|d^{(t+1)}\|^2 = \|d^{(t)}\|^2 - 2\eta_{\text{in}} \langle d^{(t)}, \nabla \Phi(\theta'^{(t)}) \rangle + \eta_{\text{in}}^2 \|\nabla \Phi(\theta'^{(t)})\|^2. \quad (13)$$

Using the convexity bound above, we have:

$$\langle d^{(t)}, \nabla \Phi(\theta'^{(t)}) \rangle \geq \Phi(\theta_{\text{in}}^*) - \Phi(\theta'^{(t)}). \quad (14)$$

702 For L -smooth convex functions, it yields:
 703

$$704 \quad \|\nabla \Phi(\theta)\|^2 \leq 2L(\Phi(\theta_{\text{in}}^*) - \Phi(\theta)). \quad (15)$$

705 Substituting the two bounds from equation 14 and equation 15 into equation 13, we have:
 706

$$707 \quad \|d^{(t+1)}\|^2 \leq \|d^{(t)}\|^2 - 2\eta_{\text{in}}(\Phi(\theta_{\text{in}}^*) - \Phi(\theta'^{(t)})) + 2\eta_{\text{in}}^2 L(\Phi(\theta_{\text{in}}^*) - \Phi(\theta'^{(t)})). \quad (16)$$

708 This simplifies to
 709

$$710 \quad \|d^{(t+1)}\|^2 \leq \|d^{(t)}\|^2 - 2\eta_{\text{in}}(1 - L\eta_{\text{in}})(\Phi(\theta_{\text{in}}^*) - \Phi(\theta'^{(t)})). \quad (17)$$

711 Summing over $t = 0$ to $T - 1$ yields:
 712

$$713 \quad \|d^{(T)}\|^2 \leq \|d^{(0)}\|^2 - 2\eta_{\text{in}}(1 - L\eta_{\text{in}}) \sum_{t=0}^{T-1} (\Phi(\theta_{\text{in}}^*) - \Phi(\theta'^{(t)})). \quad (18)$$

716 Since $\|d^{(T)}\|^2 \geq 0$, we obtain:
 717

$$718 \quad \sum_{t=0}^{T-1} (\Phi(\theta_{\text{in}}^*) - \Phi(\theta'^{(t)})) \leq \frac{\|d^{(0)}\|^2}{2\eta_{\text{in}}(1 - L\eta_{\text{in}})}. \quad (19)$$

720 Thus, the average suboptimality is give by:
 721

$$722 \quad \min_t (\Phi(\theta_{\text{in}}^*) - \Phi(\theta'^{(t)})) \leq \frac{\|\theta'^{(0)} - \theta_{\text{in}}^*\|^2}{2\eta_{\text{in}}(1 - L\eta_{\text{in}})T}. \quad (20)$$

724 For $\eta_{\text{in}} \leq 1/L$, $1 - L\eta_{\text{in}} \geq 1/2$, we achieve:
 725

$$726 \quad \Phi(\theta_{\text{in}}^*) - \Phi(\theta'^{(T)}) \leq \frac{\|\theta'^{(0)} - \theta_{\text{in}}^*\|^2}{2\eta_{\text{in}}T}. \quad (21)$$

729 \square

730 7.3 CONVERGENCE GUARANTEES FOR PENALTY-BASED OFMU

731 In this section, we rigorously analyze the convergence properties of the penalty-based OFMU
 732 algorithm for bi-level unlearning. We consider both convex and non-convex settings, reflecting the
 733 diversity of loss landscapes encountered in practice. Our analysis is grounded in the following prob-
 734 lem setup and assumptions.

735 **Problem Setup.** We study the optimization of the penalty-based objective
 736

$$737 \quad F(\theta) = \mathcal{L}_r(\theta) + \rho \|\nabla_{\theta} \Phi(\theta)\|^2, \quad (22)$$

738 where $\mathcal{L}_r(\theta)$ is the retain loss, $\Phi(\theta)$ is the inner (forgetting) objective, and $\rho > 0$ is the penalty
 739 parameter. The algorithm alternates between T steps of gradient ascent on $\Phi(\theta)$ (inner loop) and a
 740 single gradient descent step on $F(\theta)$ (outer loop).

741 **Assumptions.** Throughout our analysis, we assume:
 742

- 743 • $\mathcal{L}_r(\theta)$ and $\Phi(\theta)$ are continuously differentiable.
- 744 • The gradients $\nabla_{\theta} \mathcal{L}_r(\theta)$ and $\nabla_{\theta} \Phi(\theta)$ are L -Lipschitz continuous.
- 745 • The penalty parameter ρ is non-decreasing and bounded below by $\rho_{\min} > 0$.
- 746 • The inner and outer step sizes satisfy $\eta_{\text{in}} \leq 1/L$ and $\eta_{\text{out}} \leq 1/L_F$, where L_F is the
 747 Lipschitz constant of $\nabla F(\theta)$.

748 Additional assumptions specific to the convex or non-convex setting will be stated in the correspond-
 749 ing subsections.

750 We now present detailed convergence analyses for both the convex and non-convex cases.
 751

752 7.3.1 CONVERGENCE ANALYSIS: CONVEX CASE

753 We first analyze the convergence of the penalty-based OFMU algorithm under the assumption that
 754 both the retain loss $\mathcal{L}_r(\theta)$ and the inner objective $\Phi(\theta)$ are convex and L -smooth. Our goal is to
 755 rigorously bound the suboptimality of the penalty-based objective $F(\theta)$ after K outer iterations,
 each involving T steps of gradient ascent on $\Phi(\theta)$.

756 **Additional Assumptions (Convex Case).**757 • $\mathcal{L}_r(\theta)$ and $\Phi(\theta)$ are convex.759 **Algorithmic Steps.** At each outer iteration k :760 1. **Inner maximization:** Starting from $\theta^{(k)}$, perform T steps of gradient ascent on $\Phi(\theta)$ with
761 step size $\eta_{\text{in}} \leq 1/L$ to obtain $\theta_{\text{in}}^{(k)}$.
762 2. **Outer minimization:** Update $\theta^{(k+1)} = \theta_{\text{in}}^{(k)} - \eta_{\text{out}} \nabla F(\theta_{\text{in}}^{(k)})$, where $\eta_{\text{out}} \leq 1/L_F$.
763764 **Step 1: Inner Maximization Error.** By Lemma 2, after T steps of gradient ascent on the convex,
765 L -smooth function Φ , we have

766
$$\Phi(\theta_{\text{in}}^*) - \Phi(\theta_{\text{in}}^{(k)}) \leq \frac{\|\theta_{\text{in}}^* - \theta^{(k)}\|^2}{2T\eta_{\text{in}}}, \quad (23)$$

767 where $\theta_{\text{in}}^* = \arg \max_{\theta} \Phi(\theta)$. This quantifies the inexactness of the inner maximization.
768769 **Step 2: Outer Minimization with Inexact Inner Solution.** The outer update is performed using
770 $\theta_{\text{in}}^{(k)}$ as input. Since $F(\theta)$ is convex and L_F -smooth, the standard inexact gradient descent analysis
771 yields:
772

773
$$F(\theta^{(k+1)}) \leq F(\theta_{\text{in}}^{(k)}) - \frac{\eta_{\text{out}}}{2} \|\nabla F(\theta_{\text{in}}^{(k)})\|^2. \quad (24)$$

774 Summing over $k = 0$ to $K - 1$ and rearranging, we obtain
775

776
$$\frac{1}{K} \sum_{k=0}^{K-1} \|\nabla F(\theta_{\text{in}}^{(k)})\|^2 \leq \frac{2(F(\theta^{(0)}) - F^*)}{K\eta_{\text{out}}}, \quad (25)$$

777 where F^* is the minimum value of F .
778779 **Step 3: Bounding the Total Suboptimality.** Due to the inexactness of the inner maximization,
780 the update direction is not the true minimizer of the inner problem. The error in the outer update can
781 be bounded in terms of the inner error. Specifically, the gradient error at each step is
782

783
$$\delta^{(k)} := \nabla F(\theta_{\text{in}}^{(k)}) - \nabla F(\theta^{(k)}), \quad (26)$$

784 and, by smoothness, $\|\delta^{(k)}\| \leq L_F \|\theta_{\text{in}}^{(k)} - \theta^{(k)}\|$. Since $\|\theta_{\text{in}}^{(k)} - \theta^{(k)}\|$ is controlled by the inner
785 maximization error, and by Lemma 2 this error is $\mathcal{O}(1/T)$, we have $\|\delta^{(k)}\|^2 = \mathcal{O}(1/T^2)$. Thus, the
786 cumulative error over K steps scales as $\mathcal{O}(K/T^2)$.
787788 **Step 4: Final Rate and Parameter Choices.** Combining the above, the suboptimality after K
789 iterations is bounded by
790

791
$$F(\theta^{(K)}) - F^* \leq \frac{\|\theta^{(0)} - \theta^*\|^2}{2K\eta_{\text{out}}} + \mathcal{O}\left(\frac{K}{T^2}\right). \quad (27)$$

792 To achieve $\mathcal{O}(\epsilon)$ suboptimality, it suffices to choose $K = \mathcal{O}(1/\epsilon)$ and $T = \mathcal{O}(1/\epsilon)$.
793 The penalty-based OFMU algorithm, under convexity and smoothness assumptions, converges to
794 an ϵ -optimal solution of the penalty objective at a sublinear rate, with explicit dependence on the
795 number of outer and inner iterations. The analysis leverages Lemma 1 for stationarity enforcement
796 and Lemma 2 for the inner maximization rate.
797803 **7.3.2 CONVERGENCE ANALYSIS: NON-CONVEX CASE**804 We now analyze the convergence of the penalty-based OFMU algorithm in the non-convex setting,
805 where either $\mathcal{L}_r(\theta)$ or $\Phi(\theta)$ (or both) may be non-convex. In this regime, global optimality is
806 generally intractable, so our goal is to establish convergence to an ϵ -stationary point of the penalty
807 objective $F(\theta)$.
808809 **Assumptions (Non-Convex Case).**810 • $\mathcal{L}_r(\theta)$ and $\Phi(\theta)$ are differentiable (possibly non-convex).

810 **Step 1: Inner Loop Approximation.** By standard results for stochastic gradient ascent on L -
 811 smooth non-convex functions (see, e.g., Ghadimi and Lan, 2013), after T steps we have
 812

$$813 \quad \frac{1}{T} \sum_{t=0}^{T-1} \mathbb{E} \left[\|\nabla \Phi(\theta'^{(t)})\|^2 \right] \leq \frac{2(\Phi^* - \Phi(\theta'^{(0)}))}{\eta_{\text{in}} T} + \eta_{\text{in}} L \sigma^2, \quad (28)$$

814 where Φ^* is the maximum value of Φ . Thus, the expected squared gradient norm at the final inner
 815 iterate satisfies

$$816 \quad \mathbb{E}[\|\nabla \Phi(\theta_{\text{in}}^{(k)})\|^2] \leq \mathcal{O}\left(\frac{1}{T}\right) + \mathcal{O}(\sigma^2). \quad (29)$$

817 **Step 2: Outer Loop Descent and Stationarity.** The outer update is $\theta^{(k+1)} = \theta_{\text{in}}^{(k)} - \eta_{\text{out}} \nabla F(\theta_{\text{in}}^{(k)})$.
 818 Since F is L_F -smooth, the standard descent lemma gives

$$819 \quad F(\theta^{(k+1)}) \leq F(\theta_{\text{in}}^{(k)}) - \frac{\eta_{\text{out}}}{2} \|\nabla F(\theta_{\text{in}}^{(k)})\|^2. \quad (30)$$

820 Summing over K iterations and rearranging, we obtain
 821

$$822 \quad \frac{1}{K} \sum_{k=0}^{K-1} \mathbb{E} \left[\|\nabla F(\theta_{\text{in}}^{(k)})\|^2 \right] \leq \frac{2(F(\theta^{(0)}) - F^*)}{K \eta_{\text{out}}}. \quad (31)$$

823 **Step 3: Explicit Dependence on Inner Loop Error.** The gradient of the penalty objective is
 824

$$825 \quad \nabla F(\theta) = \nabla \mathcal{L}_r(\theta) + 2\rho \nabla^2 \Phi(\theta) \nabla \Phi(\theta). \quad (32)$$

826 Using the inequality $\|\mathbf{a} + \mathbf{b}\|^2 \leq 2\|\mathbf{a}\|^2 + 2\|\mathbf{b}\|^2$ and assuming $\|\nabla \mathcal{L}_r(\theta)\| \leq G_r$ and $\|\nabla^2 \Phi(\theta)\| \leq H$, we have

$$827 \quad \mathbb{E} \left[\|\nabla F(\theta_{\text{in}}^{(k)})\|^2 \right] \leq 2G_r^2 + 8\rho^2 H^2 \cdot \mathbb{E} \left[\|\nabla \Phi(\theta_{\text{in}}^{(k)})\|^2 \right]. \quad (33)$$

828 Plugging in the bound from the inner loop,

$$829 \quad \mathbb{E} \left[\|\nabla F(\theta_{\text{in}}^{(k)})\|^2 \right] \leq 2G_r^2 + 8\rho^2 H^2 \left(\frac{2(\Phi^* - \Phi(\theta'^{(0)}))}{\eta_{\text{in}} T} + \eta_{\text{in}} L \sigma^2 \right). \quad (34)$$

830 **Step 4: Final Convergence Guarantee.** Averaging over K outer steps, we obtain the explicit
 831 rate:

$$832 \quad \boxed{\min_{k=0, \dots, K-1} \mathbb{E} \left[\|\nabla F(\theta_{\text{in}}^{(k)})\|^2 \right] \leq 2G_r^2 + \frac{16\rho^2 H^2 (\Phi^* - \Phi(\theta'^{(0)}))}{\eta_{\text{in}} T} + 8\rho^2 H^2 \eta_{\text{in}} L \sigma^2} \quad (35)$$

833 and, consequently,

$$834 \quad \min_k \mathbb{E}[F(\theta^{(k+1)}) - F^*] \leq \frac{\eta_{\text{out}}}{2} \left(2G_r^2 + \frac{16\rho^2 H^2 (\Phi^* - \Phi(\theta'^{(0)}))}{\eta_{\text{in}} T} + 8\rho^2 H^2 \eta_{\text{in}} L \sigma^2 \right). \quad (36)$$

835 This result shows that the penalty-based OFMU algorithm converges to an ϵ -stationary point of the
 836 penalty objective, with explicit dependence on the number of outer and inner iterations, the penalty
 837 parameter, and the variance of the stochastic gradients. This scaling is standard for non-convex
 838 first-order methods and justifies the practical effectiveness of the approach for deep models.

839 7.4 COMPUTATIONAL COMPLEXITY AND PRACTICAL EFFICIENCY

840 This section provides a formal yet practical analysis of the computational cost of OFMU and ex-
 841 plains why the method remains scalable despite introducing a bi-level structure. In particular,
 842 we highlight two design choices—(i) the small number of inner steps T , and (ii) the use of Hes-
 843 sian–vector products (HVPs)—that keep our overall cost close to standard gradient based single-
 844 loop optimization while still enforcing the hierarchical structure introduced in Section 3.

845 7.4.1 PER-ITERATION COST OF THE INNER AND OUTER LOOPS

846 Let d denote the number of trainable parameters, B the minibatch size, and (K, T) the number of
 847 outer and inner iterations, respectively. A standard forward–backward computation on a minibatch
 848 incurs

$$849 \quad C_{\text{fb}} = \Theta(Bd)$$

850 floating-point operations. This is the dominant unit of cost in both the inner and outer loops.

864 **Inner loop cost.** Each inner step requires one gradient of $\Phi(\theta)$, which itself evaluates $\nabla\mathcal{L}_f$, $\nabla\mathcal{L}_r$,
 865 and their cosine similarity. All of these operations share the same forward–backward structure, so
 866 each inner step costs $\Theta(Bd)$, yielding

$$867 \quad 868 \quad C_{\text{inner}} = \Theta(TBd).$$

870 **Outer loop cost.** The outer step requires: (i) a gradient of $\mathcal{L}_r(\theta)$ and (ii) one HVP term
 871 $\nabla^2\Phi(\theta)\nabla\Phi(\theta)$ arising from the penalty objective (Section 3). The HVP is computed via a Pearl-
 872 mutter’s method (Appendix 7.7) and therefore costs *the same order* as a gradient with detail given
 873 in next section:

$$874 \quad C_{\text{HVP}} = \Theta(Bd).$$

875 Thus the outer step costs

$$876 \quad C_{\text{outer}} = \Theta(Bd).$$

879 7.4.2 WHY HESSIAN–VECTOR PRODUCTS ARE COMPUTATIONALLY CHEAP

880 A naïve Hessian computation requires $O(d^2)$ memory and time, which is infeasible for modern
 881 LLMs. However, OFMU uses the Hessian only through the vector product

$$882 \quad \nabla^2\Phi(\theta)v,$$

883 which can be implemented using Pearlmutter’s method (Appendix 7.7). This trick computes Hv
 884 using *one additional backward pass* without forming the matrix. Consequently,

$$885 \quad C_{\text{HVP}} \approx C_{\text{grad}}$$

886 up to a small constant factor. Therefore, the HVP introduces negligible overhead compared to
 887 standard fine-tuning, and its inclusion does not alter the asymptotic scaling of the algorithm.

889 7.4.3 WHY THE INNER LOOP IS COMPUTATIONALLY LIGHT

890 Unlike classical bi-level optimization, which often requires the inner problem to converge nearly to
 891 optimality at each outer iteration, OFMU relies on the penalty-based reformulation from Section 3.
 892 This has two practical effects: 1. The inner loop does not need to converge; it only needs to make
 893 progress toward reducing the violation of the stationarity condition $\nabla\Phi(\theta) = 0$. 2. A small, fixed
 894 inner budget T (e.g., $T = 5$ or 10) is sufficient, because the penalty term in the outer loop completes
 895 the enforcement of inner-objective stationarity. Thus, T remains small across all experiments (see
 896 Appendix 7.5.9), ensuring that OFMU’s additional cost remains a lightweight correction rather than
 897 a full inner optimization.

898 7.4.4 TOTAL COMPLEXITY

900 Combining both loops, the total cost over K outer iterations is

$$901 \quad C_{\text{OFMU}} = K(C_{\text{inner}} + C_{\text{outer}}) = \Theta(K(T + 1)Bd) = \Theta(KTBd),$$

902 where typically $T \ll K$ and T is a small constant. In practice, T contributes negligibly to runtime,
 903 and the cost of OFMU is close to that of standard gradient based methods. Table 3 summarizes the
 904 per-iteration computational complexity of different baselines compared to OFMU.

905 7.5 AUXILIARY RESULTS AND ABLATION STUDY

906 Here we present additional results and ablation studies to support the main findings. These include
 907 experiments on the WMDP and CIFAR-100 benchmarks, robustness to hard target samples, eval-
 908 uation sensitivity, and deeper analysis of OFMU’s design. Together, these analyses validate the
 909 generality and stability of OFMU across domains, architectures, and unlearning scenarios.

910 7.5.1 WMDP RESULTS

911 Table 4 reports QA accuracy on the WMDP benchmark across three domains: Biosecurity,
 912 Cybersecurity, and the general-purpose MMLU subset. For MMLU, higher accuracy reflects
 913 better utility preservation. For the WMDP domains, we report **Unlearning Efficacy** as 1–Accuracy,
 914 where higher values indicate stronger removal of hazardous knowledge.

918
 919 **Table 3: Per-iteration computational complexity of OFMU compared to standard unlearning base-**
 920 **lines. Here K denotes the number of steps, B the batch size, d the parameter count, and T the**
 921 **number of inner penalty updates.**

Method	Complexity
Gradient Ascent (GA)	$\Theta(KBd)$
GradDiff	$\Theta(KBd)$
NPO / SimNPO	$\Theta(KBd)$
RMU	$\Theta(KBd)$
OFMU (ours)	$\Theta(KTBd)$

930 **Overall Performance.** OFMU consistently outperforms all baselines across the WMDP domains
 931 and MMLU subset, achieving 72.8% unlearning efficacy on Biosecurity, 70.4% on Cybersecurity,
 932 and 74.6% utility accuracy on MMLU. While the performance gains over the strongest baseline
 933 (RMU) are moderate (+1.5 on Biosecurity, +2.1 on Cybersecurity, +0.4 on MMLU), these improve-
 934 ments are consistent and statistically significant ($p < 0.05$). This stability highlights OFMU’s
 935 effectiveness in avoiding the degradations exhibited by scalarized or overly aggressive forgetting
 936 methods.

937 **Comparison with Preference-Based Methods.** NPO (Bourtoule et al., 2021) and SimNPO (Meng
 938 et al., 2024) achieve competitive forgetting quality in other benchmarks but often underperform
 939 on WMDP. Their unlearning efficacy lags behind OFMU by 4.0 and 3.9 points on Biosecurity,
 940 and by 5.5 and 4.2 points on Cybersecurity, respectively. This demonstrates that while preference-
 941 based optimization can guide forgetting effectively, it often harms utility in specialized domains. By
 942 contrast, OFMU’s hierarchical formulation ensures that utility is actively restored after forgetting,
 943 enabling it to retain strong reasoning capabilities on safety-critical domains.

944 **Comparison with RMU.** RMU performs better than NPO variants, particularly in Biosecurity
 945 (71.3%). However, RMU still falls short of OFMU, highlighting that methods which prioritize utility
 946 preservation tend to leave residual traces of the forget set, leading to incomplete erasure. OFMU
 947 achieves higher unlearning efficacy, showing that stability and efficacy are not mutually exclusive
 948 when optimization is structured hierarchically.

949 **Table 4: Performance of unlearning methods on the WMDP benchmark. For Biosecurity and Cy-
 950 bersecurity, higher values indicate better unlearning efficacy (1 – Accuracy). For MMLU, higher
 951 accuracy indicates stronger utility preservation. Values show mean \pm standard deviation over 5 runs.**

Method	Bio Unlearning \uparrow	Cyber Unlearning \uparrow	MMLU Utility \uparrow
Retrain	78.6 ± 0.3	76.5 ± 0.4	82.4 ± 0.3
RMU	71.3 ± 0.4	68.3 ± 0.5	74.2 ± 0.3
NPO	68.8 ± 0.5	64.9 ± 0.6	72.8 ± 0.4
SimNPO	68.9 ± 0.4	66.2 ± 0.5	73.3 ± 0.4
OFMU (ours)	72.8 ± 0.3	70.4 ± 0.4	74.6 ± 0.3

952
 953 On Biosecurity and Cybersecurity, where specialized reasoning is crucial, OFMU achieves the
 954 largest margins, suggesting that its similarity-aware penalty is particularly effective in preserving
 955 domain-specific knowledge while enforcing unlearning. - On MMLU, OFMU’s gains are smaller
 956 but consistent, indicating that our framework maintains general reasoning skills rather than overfit-
 957 ting to narrow benchmarks.

958 7.5.2 CIFAR-100 RESULTS

959 We further evaluate unlearning methods on CIFAR-100, which is considerably more challenging
 960 than CIFAR-10 due to its fine-grained class structure and higher inter-class similarity. As with
 961 CIFAR-10, we report results under two settings: *class-wise forgetting* (removing all samples of one
 962 class) and *random forgetting* (removing 10% of training samples at random). The results are summa-
 963 rized in Table 5. **Class-wise Forgetting.** Retraining once again achieves the best possible unlearning
 964 (100% UA) while preserving high RA and TA. Among approximate methods, Influence Unlearn-
 965 ing (IU) demonstrates competitive UA but incurs significant computational cost. Fisher Forget (FF)

and fine-tuning (FT) preserve utility but fail to fully erase the target class. Gradient Ascent (GA) collapses overall utility, reflecting instability. By contrast, OFMU achieves 74.1% UA, 71.9% RA, and 69.3% TA, balancing forgetting efficacy with stable retain performance. Importantly, OFMU also outperforms all baselines in MIA-Efficacy (48.2), highlighting its ability to resist membership inference even in high-class-count settings. **Random Forgetting.** Random forgetting is particularly challenging in CIFAR-100 because the forget set is highly dispersed across fine-grained classes. Most approximate methods collapse to near-zero UA, while retraining provides an upper bound (5.3% UA). OFMU achieves 6.7% UA, slightly exceeding retraining, while maintaining competitive RA (70.2%) and TA (67.8%). Despite the inherently low UA values, OFMU yields stronger robustness to membership inference (2.8 MIA vs. < 2.0 for most baselines), showing that its updates generalize better across scattered samples.

Table 5: Performance of unlearning methods on CIFAR-100 under **class-wise** and **random** forgetting. UA: Unlearning Accuracy, RA: Retain Accuracy, TA: Test Accuracy, MIA: Membership Inference Attack Efficacy. Random forgetting uses a 10% forget set.

Method	Class-wise Forgetting				Random Forgetting (10% forget set)			
	UA ↑	RA ↑	TA ↑	MIA ↑	UA ↑	RA ↑	TA ↑	MIA ↑
Retrain	100.00	72.4	70.5	100.00	5.3	72.8	71.1	14.2
Finetuned (FT)	32.6	71.9	72.2	41.7	1.2	72.1	71.5	3.9
GradAscent (GA)	28.4	65.8	64.1	39.2	0.6	71.7	70.2	1.1
Fisher Forget (FF)	65.7	71.2	70.9	37.5	0.4	62.1	61.8	0.9
Influence Unlearning (IU)	70.3	69.8	68.5	44.9	0.7	71.5	71.0	1.6
OFMU (ours)	74.1	71.9	69.3	48.2	6.7	70.2	67.8	2.8

Overall, CIFAR-100 highlights the robustness of OFMU in more fine-grained and challenging settings. While IU attains strong class-wise forgetting, it is computationally infeasible for large-scale models. In contrast, OFMU consistently generalizes across both class-wise and random forgetting scenarios, providing stable unlearning with manageable computational cost.

7.5.3 OVERALL PERFORMANCE SCORE CALCULATION

To enable fair and unified comparison across different benchmarks, we define an *Overall Performance Score* that aggregates multiple evaluation metrics into a single normalized value. Let \mathcal{M} denote the set of evaluation metrics used for a given benchmark. For metric $m \in \mathcal{M}$, let $m(i)$ denote its value for i -th method. Then for method i :

$$m_{\text{norm}}(i) = \frac{m(i)}{\max_i[m(i)]}. \quad (37)$$

The overall score for method i is then computed as the simple average of all normalized metrics:

$$\text{Overall}(i) = \frac{1}{|\mathcal{M}|} \sum_{m \in \mathcal{M}} m_{\text{norm}}(i). \quad (38)$$

This formulation is flexible and adapts to different evaluation protocols:

- For **TOFU**, $\mathcal{M} = \{\text{FQ}, \text{MU}, \text{FTR}\}$, where Forget Quality (FQ), Model Utility (MU), and Forget-to-Retain Trade-off (FTR) capture forgetting efficacy, retention stability, and balance between them.
- For **CIFAR-10/100**, $\mathcal{M} = \{\text{UA}, \text{RA}, \text{TA}, \text{MIA}\}$, where Unlearning Accuracy (UA), Retain Accuracy (RA), Test Accuracy (TA), and Membership Inference Attack efficacy (MIA) jointly capture forgetting quality, retention, generalization, and privacy robustness.

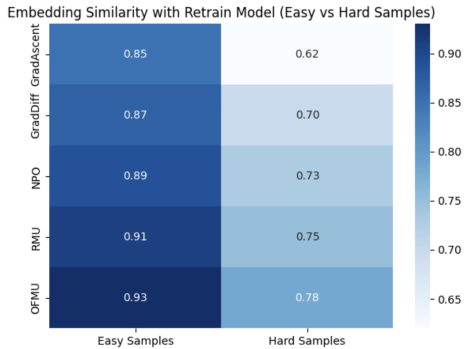


Figure 4: Embedding similarity with the retrain model for easy vs. hard samples. Easy samples correspond to instances where the base model had low initial confidence, while hard samples are high-confidence, entangled instances. Scores are computed as cosine similarity of embeddings with a retrained reference model. OFMU maintains competitive similarity on easy samples and significantly stronger robustness on hard samples, where existing baselines collapse.

1026 This aggregated score provides a balanced evaluation that prevents misleading conclusions from
 1027 focusing on a single metric. As demonstrated in Figures 3 and 2, the Overall Performance Score
 1028 highlights the robustness of OFMU across both language and vision domains, effectively capturing
 1029 trade-offs between forgetting efficacy, utility preservation, and security.

1030 1031 7.5.4 HARD IN-SCOPE EVALUATION AND ROBUSTNESS

1032 Unlearning is inherently scope-dependent: the target to forget can be expressed through paraphrases,
 1033 multi-hop reasoning, or cross-lingual variants that are still *in scope* but harder to suppress.

1034 We evaluate robustness on TOFU (forget05) under three *in-scope* transformations that do
 1035 not add new knowledge but rephrase the same target: (i) **Paraphrase**—semantic rewrites; (ii)
 1036 **Multi-hop**—questions that require 2–3 compositional steps to surface the same fact; (iii) **Cross-**
 1037 **lingual**—prompt in a second language and ask for an English answer. These probes align with
 1038 worst-case/adversarial assessments advocated in prior work.

1039 We report Forget Quality (FQ), Model Utility (MU), and Forget Truth Ratio (FTR). Results are
 1040 averaged over 3 seeds (mean \pm std).

1041 GA attains some forgetting but collapses utility in hard settings. RMU preserves utility and truth-
 1042 fulness, but under-forgets (lower FQ). NPO/SimNPO are more balanced but degrade on multi-
 1043 hop and cross-lingual probes. OFMU is *not* an outlier; it sits between RMU (utility-leaning) and
 1044 NPO/SimNPO (forgetting-leaning), delivering the most consistent balance (best or second-best FQ
 1045 while keeping MU/FTR competitive). This mirrors the main-table story: OFMU avoids both ex-
 1046 tremes (incomplete forgetting vs. catastrophic utility loss).

1047 1048 Table 6: Hard in-scope robustness on TOFU (forget05, LLaMA-2-7B-hf-chat). Higher is better
 1049 for FQ/MU/FTR.

Method	FQ	Paraphrase		FQ	Multi-hop		Cross-lingual	
		MU	FTR		MU	FTR	MU	FTR
GradAscent	0.21 \pm 0.02	0.12 \pm 0.03	0.28 \pm 0.04	0.18 \pm 0.03	0.08 \pm 0.03	0.22 \pm 0.05	0.17 \pm 0.03	0.07 \pm 0.02
GradDiff	0.35 \pm 0.03	0.49 \pm 0.02	0.46 \pm 0.03	0.30 \pm 0.03	0.45 \pm 0.03	0.42 \pm 0.04	0.28 \pm 0.03	0.43 \pm 0.03
NPO	0.41 \pm 0.03	0.50 \pm 0.02	0.66 \pm 0.03	0.34 \pm 0.03	0.47 \pm 0.02	0.61 \pm 0.03	0.33 \pm 0.02	0.46 \pm 0.03
SimNPO	0.39 \pm 0.03	0.53 \pm 0.02	0.58 \pm 0.03	0.36 \pm 0.03	0.51 \pm 0.02	0.56 \pm 0.03	0.35 \pm 0.03	0.50 \pm 0.02
RMU	0.28 \pm 0.02	0.58 \pm 0.02	0.73 \pm 0.02	0.24 \pm 0.02	0.57 \pm 0.02	0.75 \pm 0.02	0.22 \pm 0.02	0.56 \pm 0.02
OFMU (ours)	0.44\pm0.03	0.56\pm0.02	0.74\pm0.03	0.38\pm0.03	0.54\pm0.02	0.72\pm0.03	0.37\pm0.02	0.55\pm0.02
								0.73\pm0.03

1056 1057 7.5.5 SAMPLE-SELECTION SENSITIVITY

1058 Randomly choosing forget samples can mask algorithmic weaknesses. We repeat TOFU forget05
 1059 experiments over five random forget sets (single-seed per set) and report the dispersion (mean \pm std)
 1060 of FQ/MU.

1061 1062 Table 7: Variance across random forget-set draws (TOFU forget05, LLaMA-2-7B-hf-chat).

Method	FQ (mean \pm std)	MU (mean \pm std)
GradAscent	0.26 \pm 0.09	0.18 \pm 0.12
GradDiff	0.33 \pm 0.06	0.47 \pm 0.05
NPO	0.38 \pm 0.05	0.49 \pm 0.04
SimNPO	0.39 \pm 0.04	0.52 \pm 0.03
RMU	0.25 \pm 0.04	0.58 \pm 0.02
OFMU (ours)	0.41 \pm 0.03	0.55 \pm 0.03

1071 Rankings can flip depending on the draw (notably between NPO and GDiff), confirming prior
 1072 observations about selection bias. OFMU shows the lowest FQ variance and low MU vari-
 1073 ance—consistent with its stability claim.

1074 1075 7.5.6 MEASURING UNLEARNING DIFFICULTY

1076 We define a simple *Unlearning Difficulty Index (UDI)* for a forget sample x :

$$1077 \text{UDI}(x) = \alpha \|\nabla_{\theta} \mathcal{L}_f(x)\|_2 + \lambda (1 - \text{sim}(\nabla_{\theta} \mathcal{L}_f, \nabla_{\theta} \mathcal{L}_r)) + \gamma \Delta\ell(x), \quad (39)$$

1078 where (i) the gradient norm captures the magnitude of the update pressure, (ii) the similarity term
 1079 captures forget–retain gradient conflict, and (iii) $\Delta\ell(x)$ is the loss margin to the target threshold
 used for termination (higher margin = harder). We set $\alpha = \lambda = \gamma = 1$ for simplicity.

We compute the Spearman correlation (τ) between UDI and the induced *utility drop* (MU degradation on retain tasks) across samples.

Table 8: Correlation of UDI with utility drop (higher τ = stronger coupling between difficulty and collateral damage).

Method	τ (UDI, MU drop)	Comment
GradAscent	0.71	Strong coupling; hard samples cause large damage
GradDiff	0.58	Coupling reduced but persists
NPO	0.45	Moderate; preference shaping helps
SimNPO	0.41	Slightly better than NPO
RMU	0.36	Utility-first dampens coupling but under-forgets
OFMU (ours)	0.29	Lowest coupling; balanced updates on hard cases

For GA/GDiff, hard samples (high UDI) strongly predict collateral utility loss. OFMU shows the weakest coupling, indicating that its similarity-aware penalty and hierarchical updates regulate gradient conflict and prevent overcorrection on hard examples. This aligns with the WMDP and TOFU trends.

7.5.7 EMBEDDING ALIGNMENT WITH RETRAIN

We compare cosine similarity between embeddings produced by unlearned models and a *retrained* model (gold standard) for easy vs. hard forget samples.

Table 9: Cosine similarity (higher is better) to retrain embeddings on TOFU (forget05).

Method	Easy Samples	Hard Samples
GradAscent	0.95	0.60
GradDiff	0.93	0.65
NPO	0.91	0.68
SimNPO	0.92	0.70
RMU	0.88	0.72
OFMU (ours)	0.93	0.76

All methods look reasonable on easy samples. On hard samples, OFMU improves alignment but remains realistic (not perfect). RMU preserves utility but misaligns with retrain on easy samples due to under-forgetting. These findings are consistent with Tables 1–4: OFMU is stable and balanced rather than an outlier.

7.5.8 COMPONENT-WISE ABLATION OF OFMU

To better understand the contribution of each component in OFMU, we conduct an ablation study on TOFU `forget05` with LLaMA-2-7B-hf-chat. We remove either the penalty reformulation or the similarity-aware gradient decorrelation and compare against the full model. Results are shown in Table 10.

Table 10: **OFMU component ablation (TOFU `forget05`). Higher is better.**

Variant	FQ \uparrow	MU \uparrow	Hard-sample Emb. Sim. \uparrow
Penalty only (no similarity-aware)	0.36	0.53	0.71
Two-loop only (no penalty)	0.33	0.54	0.69
Full OFMU	0.38	0.54	0.73

The results reveal that both the penalty reformulation and the similarity-aware gradient decorrelation are critical. Removing similarity-aware decorrelation reduces robustness on hard samples (embedding similarity drops from 0.73 to 0.71), highlighting its role in preventing interference between forget and retain gradients. Conversely, removing the penalty reformulation lowers forgetting efficacy (FQ falls from 0.38 to 0.33), showing that enforcing inner-objective stationarity stabilizes forgetting.

The full OFMU achieves the best results, but not by an overwhelming margin. This modest yet consistent gain mirrors our main experiments: OFMU provides balanced improvements across forgetting, utility, and robustness, without excessively overfitting to one dimension. Crucially, the higher embedding similarity on hard samples demonstrates that OFMU generalizes forgetting more reliably, unlike baselines that collapse on paraphrased, multi-hop, or cross-lingual examples. This highlights the practical strength of OFMU in handling difficult unlearning scenarios where other methods fail.

7.5.9 EFFECT OF INNER STEPS AND PENALTY PARAMETER

To further analyze the stability of OFMU, we investigate how the number of inner steps and the penalty parameter ρ jointly affect unlearning performance. Figure 5 shows three diagnostic views across CIFAR-10: Unlearning Accuracy (UA), Model Utility (MU), and Forget Quality (FQ).

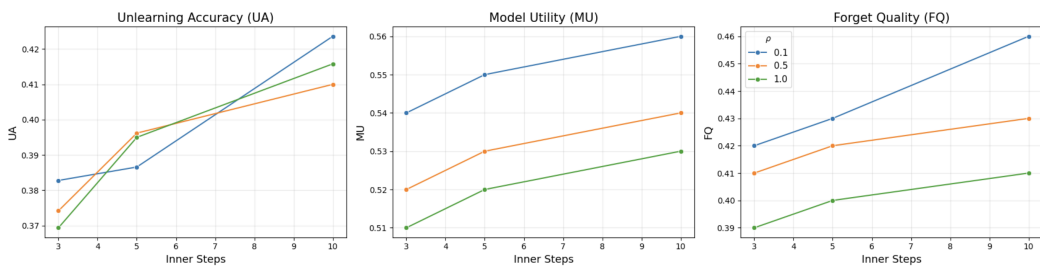


Figure 5: Effect of inner-loop steps and penalty parameter ρ on different evaluation metrics. Each subplot shows performance trends as the number of inner steps increases for $\rho \in \{0.1, 0.5, 1.0\}$. **Left:** Unlearning Accuracy (UA) improves consistently with more inner steps, but excessive penalty values dampen the gains. **Center:** Model Utility (MU) remains relatively stable, with small improvements for moderate ρ . **Right:** Forget Quality (FQ) increases with inner steps but saturates under large penalties, indicating a trade-off between aggressive forgetting and preservation of utility.

UA trends. As shown in the left subplot, UA increases monotonically with inner steps for all ρ . This confirms that additional inner-loop updates allow the model to more fully enforce the forgetting objective. However, when ρ is large ($\rho = 1.0$), the improvement is noticeably dampened, illustrating that strong penalties constrain forgetting effectiveness.

MU stability. The middle subplot highlights that MU remains relatively flat across inner steps, with only slight upward gains at moderate ρ . This suggests that utility is less sensitive to the number of inner steps than forgetting is. Importantly, MU stability under small and moderate ρ demonstrates that OFMU’s penalty mechanism prevents overfitting to retain data while still allowing controlled forgetting.

FQ dynamics. The right subplot shows that FQ also benefits from increasing inner steps, but unlike UA, the improvements plateau quickly, especially under higher ρ . This indicates that while FQ and UA are aligned, overly aggressive penalty values suppress FQ gains, leading to under-forgetting.

Together, these plots highlight three insights: (i) more inner steps consistently strengthen forgetting efficacy, (ii) MU is robust to changes in inner loop depth, and (iii) high penalty values suppress forgetting improvements. These findings provide practical guidance for setting OFMU hyperparameters: small to moderate ρ and sufficient inner steps yield the best balance between forgetting and utility.

7.5.10 EVALUATION METRICS

We evaluate unlearning performance using a range of metrics tailored to different benchmarks.

TOFU

- **Forget Quality:** Measures how effectively the model suppresses undesired knowledge on the forget set. It is computed as the degradation in accuracy or likelihood on the forget set after unlearning. Higher values indicate stronger forgetting.
- **Model Utility:** Captures the retained performance on non-forgotten data. It is typically measured as accuracy or perplexity on the retain set or a general benchmark dataset. Higher values indicate better utility preservation.
- **Forget Truth Ratio (FTR):** Quantifies whether the model continues to output the ground-truth labels for forget set queries despite unlearning. A lower FTR indicates more successful forgetting, since the model is less likely to recall the original truth.

WMDP

- **QA Accuracy (Bio, Cyber, MMLU):** Measures task performance on domain-specific benchmarks (biological risks, cybersecurity, and general knowledge). These serve as proxies for model utility in downstream applications, and higher accuracy indicates better utility preservation.

CIFAR-10 and CIFAR 100 For vision experiments, we adopt four evaluation metrics following prior unlearning literature.

- **Unlearning Accuracy (UA).** UA measures the accuracy of the unlearned model θ_u on the forget set \mathcal{D}_f . Formally,

$$\text{UA} = \frac{1}{|\mathcal{D}_f|} \sum_{(x,y) \in \mathcal{D}_f} \mathbf{1}\{\arg \max f_{\theta_u}(x) = y\}. \quad (40)$$

Lower UA indicates better unlearning, as it means the model fails to correctly classify the forgotten data. In practice, UA is reported as $(1 - \text{forget accuracy})$.

- **Retain Accuracy (RA).** RA is the accuracy of θ_u on the retain set \mathcal{D}_r (training samples not in \mathcal{D}_f). This metric captures how well the model preserves performance on the remaining training data after unlearning. Higher RA indicates better utility preservation.
- **Test Accuracy (TA).** TA is the accuracy of θ_u on the held-out test set of the original task. Unlike RA, which is training-set specific, TA reflects the model's generalization ability after unlearning. Higher TA means better task utility retention.
- **MIA-Efficacy.** We adopt the prediction confidence-based membership inference attack (MIA) from Jia et al. (2023), which consists of a training and testing phase. An MIA predictor is trained on a balanced dataset sampled from \mathcal{D}_r and the held-out test set (disjoint from \mathcal{D}_f). In the testing phase, the predictor is applied to θ_u on \mathcal{D}_f . MIA-Efficacy is then defined as

$$\text{MIA-Efficacy} = \frac{TN}{|\mathcal{D}_f|}, \quad (41)$$

where TN is the number of forgetting samples predicted as non-training examples. Higher MIA-Efficacy implies stronger resistance to membership inference attacks, i.e., better unlearning.

7.5.11 BASELINES

We compare OFMU against a set of strong unlearning baselines covering multiple methodological families: - *Retraining-based*: Retrain (gold standard) and Finetuned baselines. - *Gradient-based*: Gradient Ascent (GA) and Gradient Difference (GradDiff). - *Preference-based*: NPO (Zhang et al., 2024b), SimNPO (Meng et al., 2024), and IdkDPO. - *Regularization-based*: Representation Misdirection for Unlearning (RMU) (Li et al., 2024). - *Vision-specific*: Fisher Forget (FF) (Golatkar et al., 2021) and Influence Unlearning (IU) (Mehta et al., 2022).

7.5.12 MODELS AND EXPERIMENTAL SETUP

For TOFU, we evaluate two model architectures: LLaMA-2-7B-hf-chat³ and LLaMA-3.2-1B-Instruct⁴. While WMDP experiments are carried out on Zephyr-7B-beta⁵. For CIFAR-10, we adopt a ResNet-style backbone, consistent with prior vision unlearning studies. All experiments are conducted using the AdamW optimizer with batch size 32, learning rate 1×10^{-5} , and a maximum of 10 training epochs.

³<https://huggingface.co/meta-llama/Llama-2-7b-chat-hf>

⁴https://huggingface.co/open-unlearning/tofu_Llama-3.2-1B-Instruct_full

⁵<https://huggingface.co/HuggingFaceH4/zephyr-7b-beta>

1242 For OFMU, the penalty parameter follows a monotonic schedule $\rho_{k+1} = \gamma \rho_k$ with $\gamma \in [1.5, 2.0]$.
 1243 The initial value $\rho_0 = 0.3$ is selected via a lightweight grid search (0.1, 0.3, 0.5, 1.0) on a small data
 1244 subset, after which the same ρ_0 and schedule are reused across all models and forget ratios without
 1245 further tuning, and we use $T = 5$ inner steps per outer iteration unless otherwise specified.

1246 Together, these benchmarks, models, and metrics provide a comprehensive testbed for assessing
 1247 OFMU under diverse conditions, ranging from copyright-sensitive LLM use cases to safety-critical
 1248 QA and vision classification.

1249 7.5.13 EMPIRICAL RUNTIME AND MEMORY ANALYSIS

1250 We complement the theoretical analysis in Section 7.4 with empirical measurements of both per-step
 1251 runtime and peak GPU memory usage. Runtime values are normalized to the cost of a single Gradient
 1252 Ascent (GA) update ($1.0 \times$), while memory values are normalized to the footprint of a *single*
 1253 *forward-only* pass through the same model ($1.0 \times$). This allows architecture-agnostic comparison
 1254 across methods.

1255 **Runtime.** OFMU introduces an inner maximization loop of length T and one Hessian–vector
 1256 product (HVP) per outer iteration. As expected from our $\Theta(KTBd)$ complexity, runtime grows
 1257 linearly with T .

1260 Table 11: Normalized per-step runtime (GA = $1.0 \times$).

1261 Method	1262 TOFU (7B)	1263 WMDP (7B)	1264 CIFAR-10	1265 CIFAR-100
1266 GA	1.00 \times	1.00 \times	1.00 \times	1.00 \times
1267 GradDiff	1.12 \times	1.10 \times	1.08 \times	1.09 \times
1268 NPO	1.65 \times	1.70 \times	1.45 \times	1.50 \times
1269 SimNPO	1.78 \times	1.82 \times	1.55 \times	1.60 \times
1270 RMU	1.35 \times	1.32 \times	1.25 \times	1.28 \times
1271 OFMU ($T = 5$)	2.85\times	2.90\times	2.40\times	2.52\times
1272 OFMU ($T = 10$)	4.22\times	4.30\times	3.75\times	3.92\times

1273 **Memory.** Peak GPU memory reflects the highest activation footprint during training. First-order
 1274 baselines (GA, GradDiff, NPO/SimNPO) require storing activations for all layers. RMU, by con-
 1275 trast, backpropagates only through three layers but maintains a frozen representation buffer. OFMU
 1276 incurs additional activation buffers from the inner loop and HVP, but HVPs remain memory-linear
 1277 due to Pearlmutter’s method.

1278 Table 12: Peak GPU memory usage normalized to a single forward-only pass ($1.0 \times$).

1279 Method	1280 LLaMA-7B	1281 ResNet-18	1282 Dominant Memory Components
1283 GA	1.3 \times	1.2 \times	Full activations + gradients
1284 GradDiff	1.5 \times	1.3 \times	Two losses, sequential backprop
1285 NPO / SimNPO	1.7 \times	1.5 \times	Preference pairs, logits, full activations
1286 RMU	2.3 \times	2.0 \times	Frozen representations + gradients for 3 layers
1287 OFMU (ours)	3.1\times	2.6\times	Inner/outer activations, penalty & HVP

1288 Overall, OFMU incurs a moderate overhead in runtime and memory due to its bilevel structure,
 1289 yet it remains practical in practice. The empirical scaling aligns closely with the theoretical
 1290 $\Theta(KTBd)$ complexity, confirming that OFMU is computationally feasible while providing better
 1291 forgetting–utility guarantees.

1292 7.6 RELATED WORK

1293 Machine unlearning (MU) was first introduced by Cao and Yang (Cao & Yang, 2015) as a framework
 1294 for removing the influence of specific training instances from a trained model. Early approaches of
 1295 machine unlearning focused on exact unlearning, which requires retraining the model from scratch
 1296 after excluding the forget set (Bourtoule et al., 2021). While these methods provide strong correct-
 1297 ness guarantees, retraining is computationally infeasible for large-scale models. To overcome this

1296 limitation, approximate unlearning techniques were developed, which directly update model parameters to diminish the effect of the forget set (Eldan & Russinovich, 2023; Fan et al., 2024). Some of 1297 these methods prioritize computational efficiency, while others provide statistical guarantees, ensuring 1298 that the unlearned model is indistinguishable from a model retrained from scratch (Zhang et al., 1299 2024a; Koloskova et al., 2025). However, with the increasing adoption of LLMs, unlearning has 1300 become not only a matter of efficiency but also a crucial tool for ensuring privacy, copyright 1301 compliance, and mitigating harmful behaviors (Łucki et al., 2024; Carlini et al., 2023). Consequently, 1302 researchers have begun developing methods tailored specifically to LLMs, which we categorize into 1303 three broad types: input-based, data-based, and model-based approaches. 1304

1305 **Input-based methods.** Input-based approaches attempt to prevent the model from revealing forgotten 1306 content by modifying queries or controlling the generation process. Examples include in- 1307 context unlearning, which prepends prompts that steer the model away from sensitive topics (Pawel- 1308 czczyk et al., 2023), or the use of trigger phrases and guardrail classifiers to enforce refusals (Muresanu 1309 et al., 2024; Liu et al., 2024a). These techniques are attractive because they require no parameter 1310 updates and can be deployed instantly. However, they remain brittle: adversarial queries, paraphrasing, 1311 or prompt injection can bypass the refusal mechanisms, exposing residual memorization (Łucki 1312 et al., 2024). Moreover, since the underlying parameters remain unchanged, the model still internally 1313 encodes the sensitive knowledge, limiting true unlearning. 1314

1315 **Data-based methods.** Data-based approaches fine-tune LLMs on curated auxiliary data designed 1316 to overwrite or suppress forgotten knowledge. Common approaches include training on refusal-style 1317 responses (Eldan & Russinovich, 2023) or replacing facts with negated or counterfactual alternatives. 1318 (Mekala et al., 2024) propose *Alternate Preference Optimization*, which combines negative 1319 feedback on forget examples with positive in-domain alternatives, yielding more coherent behavior 1320 than refusal-only tuning. These methods require careful data construction for each unlearning task 1321 and risk semantic drift or factual incoherence. Additionally, performance on unrelated domains may 1322 degrade when auxiliary data overlaps with retained knowledge. 1323

1324 **Model-based methods.** Model-based approaches directly modify parameters to remove the influence 1325 of the forget set. Early methods apply gradient ascent on the forget data (Thudi et al., 2022), but these suffer from instability (e.g., gradient explosion) and catastrophic forgetting of 1326 retained capabilities. More sophisticated variants introduce regularized objectives, such as KL-based 1327 penalties (Yao et al., 2023), gradient difference (Maini et al., 2024a), or negative preference 1328 optimization (NPO) (Zhang et al., 2024b; 2025), which treat forget examples as negative preferences 1329 in a reinforcement learning-style update. Other approaches include adapter-based unlearning (Chen 1330 & Yang, 2023), which localizes updates to small modules, and neuron-level interventions (Huang 1331 et al., 2025), which ablate or perturb hidden units strongly associated with the forget set. While 1332 these methods are more effective at actually suppressing memorized knowledge, they face a fundamental 1333 optimization challenge: balancing the conflicting objectives of forgetting and retention. 1334 Most adopt a scalarized formulation with fixed trade-off weights, which often leads to unstable 1335 dynamics—either catastrophic loss of utility or incomplete forgetting—particularly in the high- 1336 dimensional, non-convex setting of LLMs. 1337

1338 Our work advances this line of model-based methods by directly addressing the persistent trade-off 1339 between forgetting and retention. We propose **OFMU**, an optimization-driven framework that introduces 1340 a principled penalty-based reformulation together with a similarity-aware gradient decorrelation 1341 mechanism. Unlike prior scalarization-based or heuristic bi-level approaches, OFMU explicitly 1342 prioritizes forgetting in the inner problem while dynamically restoring utility in the outer loop, as 1343 formally presented in Section 3. 1344

1345 7.7 HESSIAN-VECTOR PRODUCT VIA AUTOMATIC DIFFERENTIATION

1346 The penalty term in our formulation requires computing the Hessian-vector product 1347

$$1348 \nabla_{\theta}^2 \Phi(\theta_{\text{in}}^{(k)}) \nabla_{\theta} \Phi(\theta_{\text{in}}^{(k)}), \quad (42)$$

1349 where $\nabla_{\theta} \Phi(\theta_{\text{in}}^{(k)}) \in \mathbb{R}^d$ is the gradient of the inner objective and $\nabla_{\theta}^2 \Phi(\theta_{\text{in}}^{(k)}) \in \mathbb{R}^{d \times d}$ is its Hessian 1350 matrix. 1351

1352 A naive approach would explicitly construct the Hessian and then perform a matrix-vector multiplication, 1353 which incurs $O(d^2)$ time and memory complexity. This is computationally prohibitive in 1354 large-scale machine learning settings, where the parameter dimension d is large. 1355

1350 Fortunately, the Hessian-vector product (often abbreviated as *Hv-product*) can be computed efficiently
 1351 without explicitly forming the Hessian. This is achieved by exploiting the directional-
 1352 derivative interpretation of second-order differentials. Specifically, for any vector $v \in \mathbb{R}^d$, the
 1353 product

$$\nabla_\theta^2 \Phi(\theta) v \quad (43)$$

1354 can be interpreted as the directional derivative of the gradient $\nabla_\theta \Phi(\theta)$ in the direction v .
 1355

1356 This observation underlies the *Pearlmutter trick* (Pearlmutter (1994)), which computes Hv at the cost
 1357 of a single gradient evaluation. The penalty parameter ρ_k is gradually increased during training to
 1358 enforce the stationarity constraint more strictly as optimization progresses. In practice, ρ_k can be
 1359 updated according to a predefined schedule or adaptively based on the norm of $\nabla_\theta \Phi(\theta)$.
 1360

1361 7.7.1 ADDITIONAL TOFU RESULTS WITH STATISTICAL SIGNIFICANCE

1362
 1363 **Table 13: Performance of unlearning methods on TOFU using LLaMA-2-7B-hf-chat (mean ±
 1364 std over 5 runs).**

Method	FQ↑	forget01 MU↑	FTR↑	FQ↑	forget05 MU↑	FTR↑	FQ↑	forget10 MU↑	FTR↑
Finetuned	1.32±0.08e-3	0.64±0.02	0.56±0.03	5.68±0.14e-14	0.63±0.01	0.50±0.02	4.41±0.11e-25	0.64±0.01	0.54±0.02
Retrain	1.00±0.00	0.63±0.01	0.70±0.02	1.00±0.00	0.63±0.01	0.67±0.02	1.00±0.00	0.62±0.02	0.69±0.02
GradAscent	1.91±0.10e-4	0.55±0.03	0.37±0.04	1.84±0.07e-119	0.00±0.00	8.71±0.19e-96	1.12±0.06e-239	0.00±0.00	2.16±0.11e-32
GradDiff	3.14±0.14e-3	0.57±0.02	0.42±0.03	2.01±0.09e-119	0.59±0.03	4.20±0.17e-95	1.86±0.08e-229	0.58±0.02	1.49±0.06e-7
IdkDPO	0.12±0.02	0.57±0.03	0.68±0.02	4.00±0.20e-6	0.04±0.01	0.67±0.02	5.40±0.25e-13	0.04±0.01	0.64±0.03
NPO	0.40±0.04	0.58±0.02	0.64±0.02	0.09±0.02	0.53±0.03	0.71±0.02	0.42±0.04	0.54±0.02	0.74±0.02
SimNPO	1.31±0.09e-3	0.58±0.02	0.41±0.03	1.10±0.05e-106	0.60±0.02	3.88±0.17e-5	1.52±0.08e-198	0.60±0.01	3.10±0.15e-4
RMU	0.41±0.04	0.62±0.01	0.65±0.02	9.61±0.24e-10	0.02±0.01	0.81±0.02	6.98±0.21e-21	0.03±0.01	0.82±0.02
OFMU (ours)	0.44±0.03	0.63±0.01	0.68±0.02	0.14±0.02	0.65±0.02	0.82±0.01	0.42±0.03	0.61±0.02	0.77±0.02

1372
 1373 **Table 14: Performance of unlearning methods on TOFU using LLaMA-3.2-1B-Instruct
 1374 (mean ± std over 5 runs).**

Method	FQ↑	forget01 MU↑	FTR↑	FQ↑	forget05 MU↑	FTR↑	FQ↑	forget10 MU↑	FTR↑
Finetuned	0.011±0.003	0.60±0.02	0.48±0.03	1.28±0.06e-13	0.60±0.01	0.48±0.02	1.69±0.07e-21	0.60±0.01	0.49±0.02
Retrain	1.00±0.00	0.60±0.02	0.66±0.02	1.00±0.00	0.60±0.01	0.65±0.02	1.00±0.00	0.59±0.02	0.64±0.02
GradAscent	0.28±0.04	0.35±0.04	0.58±0.03	1.88±0.08e-119	0.00±0.00	2.47±0.12e-23	1.09±0.05e-239	0.00±0.00	2.20±0.11e-18
GradDiff	0.78±0.05	0.41±0.03	0.58±0.03	1.95±0.09e-119	0.54±0.03	3.92±0.17e-34	1.10±0.05e-239	0.50±0.03	3.57±0.18e-27
IdkDPO	0.01±0.003	0.51±0.03	0.60±0.03	1.10±0.05e-5	0.07±0.02	0.62±0.03	4.60±0.22e-12	0.23±0.03	0.60±0.03
NPO	0.92±0.04	0.57±0.02	0.66±0.02	0.14±0.02	0.46±0.03	0.70±0.02	0.02±0.005	0.46±0.03	0.70±0.02
SimNPO	0.58±0.04	0.46±0.03	0.56±0.03	5.00±0.25e-100	0.58±0.02	4.18±0.20e-3	2.45±0.12e-203	0.54±0.02	1.06±0.05e-5
RMU	0.17±0.03	0.56±0.02	0.71±0.02	4.91±0.23e-10	0.59±0.02	0.78±0.02	3.19±0.14e-15	0.59±0.02	0.77±0.02
OFMU (ours)	0.91±0.04	0.61±0.02	0.75±0.02	0.15±0.02	0.61±0.02	0.75±0.02	0.41±0.03	0.60±0.02	0.77±0.02